Phytomedicine Plus 4 (2024) 100639

Contents lists available at ScienceDirect

Phytomedicine Plus

journal homepage: www.sciencedirect.com/journal/phytomedicine-plus

In vitro hypoglycemic, antioxidant, anti-inflammatory activities and phytochemical profiling of aqueous and ethanol extracts of *Helichrysum cymosum*

Achasih Quinta Nkemzi [a], Kunle Okaiyeto [a], Nasifu Kerebba [b], Fanie Rautenbach [c], Omolola Oyenihi [a], Okobi Eko Ekpo [d], Oluwafemi O. Oguntibeju [a,*]

[a] *Phytomedicine and Phytochemistry Group, Department of Biomedical Sciences, Faculty of Health and Wellness Sciences, Cape Peninsula University of Technology, Bellville 7535, South Africa*
[b] *Department of Chemistry, Makerere University, Kampala 7062, Uganda*
[c] *Applied Microbial and Health Biotechnology Institute, Cape Peninsula University of Technology, Cape Town 7530, South Africa*
[d] *Department of Biological Sciences, College of Medicine and Health Sciences, Khalifa University, Abu Dhabi P.O. Box 127788, UAE*

ARTICLE INFO

Keywords:
Diabetes mellitus
Glucose utilization
Metabolic disorder
Phytochemical compounds
A-amylase, α-glucosidase

ABSTRACT

Background: Diabetes mellitus (DM) is a complicated and multifaceted metabolic disorder that poses significant health challenges for individuals and healthcare systems worldwide. Efforts to understand its pathophysiology and develop novel treatment options for the disease through preclinical research and drug discovery have been the focus of several researchers globally. One of the approaches to tackle this is the use of plant-based products, which are therapeutically effective and affordable.

Purpose: The current study investigated the phytochemical constituents of *Helichrysum. cymosum* aqueous (AQ) and 70% ethanol (ET) extracts, their cytotoxicity, as well as their in vitro antidiabetic effects via antioxidant, anti-inflammatory, and selected enzyme inhibition assays.

Materials and methods: Bioactive compounds were identified using High-Performance Liquid Chromatography and UHPLC-ESI-MS. Cytotoxicity was assessed on C3A hepatocyte cells using MTT (3-(4,5-Dimethylthiazol-2-yl)-2,5-diphenyl tetrazolium bromide). Antioxidant activity was determined using the average cellular CellROX® Orange fluorescent intensity, ferric reducing antioxidant power (FRAP), trolox equivalent antioxidant capacity (TEAC) and 2, 2-diphenyl-1-picrylhydrazyl (DPPH) radical scavenging assay. The mouse macrophage cell line, RAW 264.7 was used to assess anti-inflammatory activity by measuring the levels of nitrite produced. Enzymatic inhibitory assays such as alpha glucosidase, alpha amylase and pancreatic lipase inhibition were performed to determine the antidiabetic effect of the plant extracts. Also glucose uptake and glucose utilization on C3A hepatocytes and L6myocytes were evaluated.

Results: The results show significantly higher polyphenol and flavonol contents in ET (303 ± 4 mg GAE/g, 183 ± 6 mg QE/g, respectively) compared to AQ (83.7 ± 2 GAE/g, 36.0 ± 1 respectively). ET also showed significantly higher antioxidant activity (DPPH assay: 1893 ± 34 μmol TE/g; FRAP assay: 158 ± 2 μmol AEE/g; and ABTS assay: 1402 ± 26 μmol TE/g) compared with AQ (DPPH assay: 606 ± 8.4 μmol TE/g; FRAP assay: 530 ± 2 μmol AEE/g; and ABTS assay: 450 ± 11 μmol TE/g). HPLC reveals the presence of caffeic acid (AQ), chlorogenic acid (AQ and ET), kaempferol (AQ), and rutin (ET), while UHPLC-ESI-MS analysis identified 43 compounds in both AQ and ET. Cytotoxicity was observed only for ET at a concentration of 250 μg/mL, while both AQ and ET exhibited cellular antioxidant activity, alpha-glucosidase activity, and minor alpha-amylase activity. There was

Abbreviation: ANOVA, analysis of variance; AME, accurate mass match error; AQ, aqueous extract; AAE, ascorbic acid equivalent; DM, diabetes mellitus; DMSO, dimethylsulfoxide; DMEM, Dulbecco's modified eagle medium; DNS, 3,5-dinitrosalicylic acid, ET, ethanol extracts; HPLC, high-pressure liquid chromatography; GAE, gallic acid equivalent; LPS, lipopolysaccharide liquid chromatography mass spectroscopy; MEM, minimal essential medium; MTT, 3-(4,5-Dimethylthiazol-2-yl)-2,5-diphenyl tetrazolium bromide; NED, N-(1-Naphtyl)-ethylenediamine dihydrochloride; PBS, phosphate-buffered saline; ROS, reactive oxygen species;. T1D, type 1 diabetes; T2D, type 2 diabetes; TE, trolox equivalent; UHPLC-MS, ultra-high performance; QE, quercetin equivalent.

* Corresponding author at: Department of Biomedical Sciences, Faculty of Health and Wellness Sciences, Cape Peninsula University of Technology, Bellville 7535, South Africa.

E-mail address: oguntibejuo@cput.ac.za (O.O. Oguntibeju).

https://doi.org/10.1016/j.phyplu.2024.100639

Available online 16 September 2024

also significant glucose uptake and its utilization by C3A hepatocytes and L6 myocyte cells. However, the extracts did not exert substantial effect on lipase inhibition in the current study.
Conclusion: The finding reveals that the bioactive compounds present in *H. cymosum* extracts have potential antioxidant, anti-inflammatory, and hypoglycemic effects; therefore, these compounds can be further explored as future candidates for drug discovery.

1. Introduction

Diabetes mellitus is a complicated chronic metabolic disease represented by hyperglycemia, emanating from carbohydrates, fats, and protein metabolism (Oguntibeju, 2019; Nasab et al., 2020; Dilworth et al., 2021). Hyperglycemia is caused by disrupted insulin production or secretion (Akinyede et al., 2021a). DM is a major public health concern in underdeveloped and developed nations, with a reported incidence of about 451 million individuals conceivably existing with DM, and 693 million people have been projected to be affected by DM by 2045 (Jadalla et al., 2022). The etiology of hyperglycemia in DM is connected to oxidative stress (OS) and inflammation (Papachristoforou et al., 2020). Oxidative stress is created by an imbalance between excess production and elimination of reactive oxygen species (ROS) beyond the body's natural antioxidant capacity (Omodanisi et al., 2017). ROS production is generated from increased inflammatory mediators and protein glycosylation, the autoxidation of glucose, the formation of superoxide radicals, and advanced glycation byproducts resulting in the alteration of cellular hemeostasis (Omodanisi et al., 2017; González et al., 2023; Sadiq, 2023). Persistent hyperglycemia has a profound impact on the body organs, leading to a wide range of complications like cardiovascular disease, kidney failure, heart attack and stroke, arterial disease, and damage to peripheral nerves (Akinfenwa et al., 2022; Maniruzzaman et al., 2020). The long-term effects of diabetic complications are associated with uninterrupted OS in diabetic cells and hyperpolarization (Dilworth et al., 2021).

Primary intervention in treating DM necessitates regulation of hyperglycemia and decreasing OS and inflammation outcomes (Wang et al., 2021). Therefore, inhibition of key digestive enzymes such as α-glucosidase, α-amylase, and pancreatic lipase plays a beneficial role in the treatment of DM and obesity (Dirir et al., 2022; Liu et al., 2020). Current treatments for DM have been achieved using oral hypoglycemic medications, insulin therapy, management of food intake, and physical exercises, among others (Dilworth et al., 2021; Prasathkumar et al., 2022; Dumbre et al., 2023). However, most DM therapies are known to have undesirable outcomes and are relatively expensive, thereby hampering their use by many people with diabetes (Akinfenwa et al., 2022). It is important to search for an alternative treatment option with minimal side effects and that is more cost effective. Natural remedies have been identified as treatment options to manage DM in most developing countries and several bioactive constituents have been documented and reported to be essential to the treatment realization of DM (Tran et al., 2020; Ansari et al., 2022; Sagbo and Hussein, 2022). Compounds like alkaloids, flavonoids, polyphenols, and tannins, are known to be instrumental in glucose regulation and alleviating hyperglycemic effects (Akinfenwa et al., 2022). Flavonoids obtained from plant extracts have been observed to exhibit antidiabetic properties by inhibiting the action of carbohydrate digestive enzymes (α-glucosidase and α-amylase enzymes) associated with hyperglycemia (Tran et al., 2020; Amoo et al., 2022; Jadalla et al., 2022).

"The genus *Helichrysum* Mill belong to the family Asteraceae, with a global estimate of 500–600species, 250 of which are of South African origin" (Lourens et al., 2008). Species within this genus are scented, woolly shrubs with a golden yellow flower (Matanzima, 2014; Leonardi et al., 2018). The species *Helichrysum cymosum,* which is used within the rural communities of South Africa as an herbal remedy to treat diseases like coughs, colds, pains, infected wounds, and headaches, has also been reported to induce trances and attract goodwill from ancestors (Heyman, 2013; Maroyi, 2019). Other therapeutic applications include cardiovascular complications, kidney problems, urinary infections, eye infections, vomiting, insomnia, diarrhea, laxatives, blocked noses, as an immune system booster, for controlling flatulence, for weak bones, as an insect repellant, for skin infections, and for treating varicose veins and influenza (Jadalla et al., 2022). Ealier studies have reported antioxidant, anti-inflammatory, antifungal, antiviral, antimicrobial, anti-diabetic, and cytotoxic effects (Jadalla et al., 2022). Bioactive compounds such as sesquiterpenes and chalcones have been isolated from this species (Matanzima, 2014; Maroyi, 2019; Jadalla et al., 2022). Despite their promising therapeutic potential, a complete spectrum of phytochemical compounds and their biological activities, such as antidiabetic, antioxidant, and anti-inflammatory have not been fully investigated and comprehended. It is based on this background that our research seeks to investigate the effect of aqueous and ethanol extracts on the major digestive enzymes α-amylase, α-glucosidase, and pancreatic lipase, as well as their antidiabetic, antioxidant and anti-inflammatory potential of the isolated bioactive compounds from the extracts.

2. Materials and methods

2.1. Reagents

RAW 264.7 mouse macrophages were purchased from Cellonex (South Africa). Sulfanilamide Solution and N-(1-Naphtyl)-ethylenediamine dihydrochloride (NED) Solution were made following the manufacturer's instructions and products purchased from Promega. Lipopolysaccharide (LPS) and aminoguanidine were purchased from Sigma-Aldrich (St. Louise, MO, USA). RPMI-1640 culture medium and fetal bovine serum (FBS) were purchased from GE Healthcare Life Sciences (Logan, UT, USA). Minimal Essential Medium (MEM) and phosphate-buffered saline (PBS) with and without Ca^{2+} and Mg^{2+} were purchased from Cytiva (Marlborough, MA, USA). Bis-benzamide H33342 trihydrochloride (Hoechst), non-essential amino acids, and penicillin/streptomycin were purchased from Sigma-Aldrich (St. Louis, MO, USA). CellROX® Orange reagent was purchased from Thermo Fisher Scientific (Waltham, MA, USA). A-amylase type VI-B from Porcine pancreas, acarbose, starch, 3,5-dinitro salicyclic acid, sodium monobasic and diabasic, alpha-glucosidase from *Sacchromyces cerevisiae, and* pNPG were all purchased from Sigma-Aldrich (St. Louis, MO, USA). MTT (3-(4,5-dimethylthiazol-2-yl)-2,5-diphenyl tetrazolium bromide) and Dulbecco's Modified Eagle Medium (DMEM) were procured from GE Healthcare Life Sciences (Logan, UT, USA). All solutions were prepared freshly when needed for the respective assays, unless stated otherwise.

2.2. Plant collection

Helichrysum cymosum shoots were harvested in the garden of the Cape Peninsula University of Technology, Bellville campus, Cape Town, South Africa. The plant was authenticated by a botanist (P. Dryfhout) with voucher number 3708 and stored in the herbarium at the Department of Horticultural Sciences, Cape Peninsula University of Technology, Western Cape, South Africa. All experimental protocols and procedures of the study were approved by the Research Ethics Committee (REC) of the Faculty of Health and Wellness Sciences, Cape Peninsula University of Technology, South Africa (ethics approval number *CPUT/HWS-REC2021/H1*).

2.3. Extraction preparation

The shoots of *H. cymosum* were washed thoroughly, cleaned, and dried in an oven at 40 °C. The extraction protocol was according to Aladejana et al. (2020), with slight changes. The plants were then crushed to powder using an electric grinder. Subsequently, 200 g of crushed samples were soaked in 2.5 L of 70% ethanol and distilled water, respectively, and then stirred for 48 h. The extracting solvent, 70% ethanol, was used because it has been reported to give a high yield of phytochemicals (Tourabi et al., 2023). Both ethanol and aqueous extracts were then filtered using a funnel and Whatman No. 1 filter paper. The ethanol extract was concentrated at 70 °C using a rotary vacuum evaporator, while the aqueous extract was freeze-dried. The concentrated extracts were stored at 4 °C in the refrigerator until required.

2.4. Cell culture maintenance

Human hepatoma-derived C3A hepatocytes were purchased from the American Type Culture Collection and maintained in 10 cm culture dishes in complete medium (MEM with 1% non-essential amino acids, 10% FBS, penicillin/streptomycin). The cells were incubated at 37 °C with 5% CO_2 in a humidified environment and sub-cultured after 90% confluence. Test samples of the plant extracts were prepared by reconstituting in dimethyl sulfoxide (DMSO) 100 mg/mL, then sonicated and stored at 4 °C until used.

2.5. MTT cytotoxicity assay

Cytotoxicity analysis was performed following the procedure in Okaiyeto et al. (2022a) with slight modifications. This analysis was performed to establish a safer concentration of the extracts for subsequent assays. C3A hepatocyte cells were seeded in 96 well plates at 5000 cells/well (100 µL aliquots) and left overnight to attach (24 h). Five hundred (500) µg/mL dilutions of each extract were prepared independently in a complete medium and a 6-point serial dilution was made with the following concentrations: 15.6 µg/mL, 31.25 µg/mL, 62.5 µg/mL, 125 µg/mL, 250 µg/mL, and 500 µg/mL. From each dilution, 100 µL aliquots were added to 100 µL of attached cells in the 96 well plate, thus yielding final concentrations of 7.8 µg/mL, 15.6 µg/mL, 31.25 µg/mL, 62.5 µg/mL, 125 µg/mL, and 250 µg/mL. The cells were treated for 48 h at 37 °C, 5% CO_2, and 30 µM Melphalan (100 mM stock) was used as a positive control. The Treatments were aspirated from the wells and 100 µL MTT (0.5 mg/mL) in the complete medium was added to each well and cells were incubated for 3 h. After that, 100 µL DMSO was added to each well, and absorbance was measured at 540 nm using a BioTek® PowerWave XS spectrophotometer (Winooski, VT, USA). The graphs of the percentage cytotoxicity against the concentrations of the extracts were plotted using GraphPad Prism 5.

2.6. Cellular antioxidant assay

The cellular antioxidant activity (CAA) was assessed according to the procedure described by Wolfe and Liu. (2007). The assay was used to quantify the antioxidant activity of phytochemicals in food extracts and dietary supplements in live cells using an oxidant in conjunction with a fluorescent probe specific for the detection of reactive oxygen species (ROS). The experimental design discussed below is such that the observed activity reflects both the direct ROS scavenging activity of the sample as well as potential changes in the inherent capacity of the cells to resist oxidative stress, as cells were pre-treated with the sample for 24 h before exposure to TBHP.

The C3A hepatocytes were seeded in 96-well plates at a density of 2×10^4 cells/well in 100 µL aliquots and left overnight to attach. Afterward, treatments were prepared in a complete medium and added to the cells, and 100 µM catechin was added as a positive control and incubated for 24 h. Oxidative stress was induced by adding tert-butyl hydroperoxide (TBHP) to the culture/treatment medium at a final concentration of 30 µM and incubating for 2 h. The culture/treatment medium was gently aspirated, and 100 µL of staining solution [CellROX® Orange (5 µM) and Hoechst 33,342 (5 µg/mL) in PBS with Ca^{2+} and Mg^{2+}] was added to each well. Plates were incubated for 30 min (protected from light), and fluorescent micrographs were captured immediately using an ImageXpress Micro XLS Widefield Microscope (Molecular Devices) with a 10x Plan Fluor objective using DAPI and TRITC (tetramethylrhodamine isothiocyanate) filter cubes. Acquired images were analyzed using the MetaXpress software and the Multi-Wavelength Cell Scoring Application Module. Antioxidant activity was determined using the average cellular CellROX® orange fluorescent intensity. All values obtained were calculated using GraphPad Prism 5.

2.7. Anti-inflammatory activity

Anti-inflammatory analysis was conducted according to the procedure of Shauli et al. (2023) with minor changes. The RAW 264.7 cells were seeded in RPMI1640 culture medium supplemented with 10% FBS (RPMI complete medium) into 96-well plates at a density of 1×10^5 cells per well and allowed to attach overnight.

The following day, the spent culture medium was removed and 50 µL sample aliquots (diluted in RPMI complete medium) were added to give final concentrations of 50, 100, and 200 µg/mL. To assess the anti-inflammatory activity, 50 µL of LPS (final concentration of 500 µg/mL)-containing medium was added to the corresponding wells. Aminoguanidine (AG) was used as the positive control at 100 µM, and cells were incubated for a further 24 h. To quantify NO production, 50 µL of the spent culture medium was transferred to a new 96-well plate. Sulfanilamide solution and NED solution were prepared as per the manufacturer's instructions. A 50 µL Sulfanilamide solution was added to the spent culture medium and incubated for 10 min in the dark at room temperature. Fifty (50) µL NED solution was then added to each well and further incubated for 5–10 min in the dark at room temperature. The absorbance was measured at 540 nm (BioTek® PowerWave XS spectrophotometer), and a nitrite standard curve (using sodium nitrite dissolved in a culture medium) was used to determine the concentration of NO in each sample.

2.8. Determination of hypoglycaemic effect

2.8.1. Alpha amylase inhibitory activity

Alpha amylase activity was determined as described in Aladejana et al. (2020), using the 3,5-dinitrosalicylic acid (DNS) method with slight modifications. Both aqueous and ethanol extracts were dissolved in their various solvents. Different concentrations (10, 50, 100, 250, 500, and 1000 µg/mL) of the plant extracts were placed in test tubes (40 µl) each. Into the extract solutions, 160 µl of distilled water were added. Afterward, 400 µl of starch solution (0.5 g starch in 50 ml phosphate buffer) was added into the test tubes to initiate the reaction. Subsequently, 200 µl of α-amylase (4 units/ml) was incubated at 35 °C for 10 min to start the reaction. From the incubated solution, 200 µl was placed in a different test tube, and 100 µl of DNS (20 mL of 30 g of sodium potassium tartrate tetrahydrate mixed with 50 mL of 1 g of 3,5-dinitrosalicylic acid solution and 20 ml of 2 M NaOH at 90–95 °C) was added to end the reaction and boiled for 15 min. The mixed solution was then cooled down to a normal temperature, and 900 µl of distilled water was used to dilute the solution. The sample blank was prepared using a similar concentration of the plant extracts without the enzymes, and another blank with 100% enzyme activity was prepared with buffer in place of the plant extract. Acarbose was used as a positive control and was prepared similarly to the test samples, as described above. From the test sample, blanks, and positive control, 200 µl of each mixture was placed in a 96-well plate, and the absorbance was measured at 540 nm using a UV spectrophotometer. The percentage inhibition of the enzyme

α-amylase was determined using the equation (As-Ac/Ac) x 100.

2.8.2. Alpha-glucosidase activity

Alpha-glucosidase activities of aqueous and ethanol extracts of *H. cymosum* were evaluated following the procedure described by Erukainure (2018) with minor modifications. Briefly, 50µl of both plant extracts at different concentrations (10, 50, 100, 250, 500, and 1000 µg/mL) and α-glucosidase from *Sacchromyces cerevisiae* (1.0 Unit/mL) were prepared in phosphate buffer 100 mM at pH 6.8, placed in a 96-well plate, and incubated for 15 min at 37 °C. Afterward, 100 µL of 5 mM p-Nitrophenyl-α-d-glucopyranoside (pNPG) solution prepared in phosphate buffer (100 mM, pH 6.8) was added to the reaction mixture and incubated for an additional 20 min at 37 °C. Acarbose was used as a positive control, and the absorbance was measured at 405 nm. The percentage inhibition was calculated with the formula below:

$$\%\ alpha\ glucosidase\ inhibition = \frac{(\text{absorbance of control} - \text{absorbance of test sample})}{\text{absorbance of control}}\ \text{X } 100$$

2.8.3. Glucose uptake and utilization

Glucose uptake and its utilization were evaluated using C3A hepatocytes and L6 myocytes following the procedure in van de Venter et al. (2008), with some modifications. Both cells (C3A hepatocytes and L6 myocytes) were seeded, respectively, in 96-well plates (2×10^4 cells/-well, 100 µL aliquots) and left overnight to attach. Various concentrations of treatments were prepared in a complete medium and added to the cells, followed by incubation for 24 h (two plates) and 48 h (two plates) for each cell type. After 24 and 48 h of incubation, cell culture/treatment medium (5 µL for C3A; 10 µL for L6), was removed from the respective plates and transferred into new 96 well plates (A), which were sealed and stored at -20 °C until required. The rest of the medium was aspirated, and cells were washed with 100 µL PBS and 25 µL of incubation buffer (RPMI-1640 diluted with PBS containing 0.1% bovine serum albumin (BSA) to a final glucose concentration of 8 mM) was added to cells (C3A and L6). Insulin (1 µg/mL) was used as a positive control, and the cells were then incubated for another 4 h. Some of the culture medium (5 µL) was transferred to a new 96-well (plate B). Afterward, 200 µL of glucose oxidase reagent (3 mM phenol, 0.4 mM 4-aminoantipyrine, 0.25 mM EDTA, and 2.5 U/mL horseradish peroxidase in 0.5 M PBS (pH 7.0) with 1 mU/mL glucose oxidase from *Aspergillus niger*) was added to the plates (A and B), respectively, and incubated for 15 min at room temperature. Cell-free wells containing incubation buffer and complete culture medium were used as glucose standards. The absorbance was then measured at 510 nm using a BioTek® PowerWave XS spectrophotometer (Winooski, VT, USA). Glucose uptake and consumption were determined as a function of the concentration of glucose (mM) remaining and expressed as the difference between the mean of the standard and test samples. The MTT assay was further used to determine cell viability during the analysis.

2.8.4. Pancreatic lipase inhibition

Pancreatic lipase inhibition for the aqueous and ethanol extracts was performed following the procedure described by Pringle et al. (2021). Different concentrations of sample extracts were established at 500, 250, 125, 62.5, and 31.25 µg/mL. A volume of 10 µL of the extracts and 5 µL of porcine pancreatic lipase enzyme (100 mg mL^{-1} prepared in 100 mM Tris–HCl, pH 8.0) were pre-incubated at 37 °C for 15 min. Subsequently, 170 µL of the substrate (*p*-nitrophenyl palmitate (pNPP) [1 mg/mL in isopropanol), with reaction buffer (gum arabic (1 mg mL^{-1}), sodium deoxycholate (2 mg mL^{-1}) and Triton X-100 (5 µL per mL) prepared in 100 mM Tris–HCl (pH 8.0)] was added to the mixture containing extracts and enzymes and incubated at 37 °C for 25 min. Pancreatic lipase activity was then determined by measuring the absorbance at 405 nm using a BioTek® PowerWave XS spectrophotometer, and 100 µM Orlistat was prepared and used as a positive control. The percentage of pancreatic lipase inhibition was calculated according to the equation:

$$\%\ Lipase\ inhibition = \frac{\text{A405nm of blank} - \text{A405nm of test sample})}{\text{A405nm of blank}}\ X\ 100$$

2.9. Phytochemical screening and antioxidant properties of aqueous and ethanol extracts of Helichrysum cymosum (HC)

2.9.1. Determination of total polyphenols content (TPC) of H. cymosum

The total polyphenol content of the aqueous and ethanol extracts of the plant was determined using the Folin-Ciocalteu method described by Singleton et al. (1999). Briefly, 25 µL of the extract solution was mixed with 25 µL of Folin-Ciocalteu reagent (0.1 M) and 100 µL of 7.5% Na_2CO_3 in a 96-well plate and then incubated for 30 min at room temperature. The absorbance was measured at 765 nm. TPC was estimated using gallic acid as standard and results were expressed as milligram of gallic acid equivalents per 1 gram of dry weight (mg GAE/g dry weight).

2.9.2. Determination of total flavonol content (TFC)

Total flavonols for both aqueous and ethanol extracts were determined according to the procedure by Mazza et al. (1999). Into each well plate, 12.5 µL of the extracts, 12.5 µl of 0.1% HCl in 95% EtOH, and 225 µl of 2% HCl were added, while quercetin was used as the standard. The plate was left for 30 min at room temperature, and absorbance was measured at 360 nm. All results were expressed as milligrams of quercetin equivalents per gram (mg QE/g).

2.9.3. Determination of flavanol content

The flavanol content of the AQ and EtOH extracts was determined as described by McMurrough and McDowell (1978) using a calorimetric procedure, whereby the flavanols in the extracts react with 4-(Dimethylamino)-cinnamaldehyde giving a light blue coloration. Catechin was used as standard, and the plate was kept for 30 min, after which absorbance was measured at 640 nm. Results were expressed as milligrams of catechin equivalents per gram (mg CE/g).

2.9.4. Ferric reducing antioxidant power (FRAP)

The FRAP assay was performed to determine the total antioxidant capacity of *H. cymosum* aqueous and ethanol extracts. The experimental procedure for this assay was adopted from Benzie and Strain (1996). The plant extract (0.05 g) was weighed and dissolved in 60% ethanol and centrifuged for 1 min at 4000 rpm after which 10 µL of extracts at different concentrations were placed in triplicate in each well, and 300 µL of FRAP reagent (10 mM 2, 4, 6-tripyridyl-s-triazine (TPTZ), 20 mM $FeCl_3$, and acetate buffer (pH 3.6)) was added into the same wells. Ascorbic acid was used as a standard, and the plates containing the samples and standard were incubated for 30 min at 37 °C and the absorbance reading was later measured at 593 nm. All the results were expressed as µM ascorbic acid equivalent per gram dry weight (µmol AAE/g).

2.9.5. Trolox equivalent antioxidant capacity (TEAC)

TEAC analysis measures the capacity of antioxidants to scavenge ABTS (2, 2′-azino-bis (3-ethylbenzothiazoline-6-sulphonic acid) radical cation, according to the method in Re et al. (1999). An ABTS stock solution containing (8 mM ABTS and 3 mM potassium persulfate) was prepared 24 h before the experiment. ABTS reagent mix 275 µL and 25 µL of extract samples were placed into the 96 well plates, and Trolox was used as a standard. This was incubated for 30 min, and the absorbance was read at 734 nm using a plate reader. TEAC results were expressed as µmol TE/g.

2.9.6. The 2, 2-diphenyl-1-picrylhydrazyl (DPPH) radical scavenging assay

The DPPH assay of *H. cymosum* was determined according to the procedure in Sharma and Bhat (2009) with some modifications. Different concentrations of the extracts were diluted, and 25 µL of each dilution was placed into a 96-well plate in triplicate. Afterward, 275 µL of freshly prepared DPPH solution (24 mg DPPH with 100 mL methanol) was added to each well. The mixture was incubated in the dark for 30 min, and the absorbance was measured at 517 nm using a microplate reader. Trolox was used as a standard, and measurements were recorded as (µmol TE/g).

2.9.7. High-Performance liquid chromatography (HPLC)

The phenolic acid and flavonoid content of the aqueous and ethanoic extracts of *H. cymosum* were determined by high-performance liquid chromatography (HPLC) (Agilent Technology 1200 series, Bellefonte, USA) using a diode array detector and a C18 column (5 µm (4.6 mm x 150 mm i.d.). Briefly, into the HPLC column 20 µl of samples were automatically injected, and the mobile phase composition consisted of 0.1% acetic acid in water (A) and 0.1% Acetic acid in methanol (B) at a flow rate of 1 mL/min. A gradient elution was performed, running from 80:20 (A: B) to 20:80 (A: B) over 30 min. Compound detection was done at 320 nm and 360 nm, with the peaks of specific phenolic acid and flavonoid standards being documented based on retention time (Vongsak et al., 2012). The calculation for the concentration was obtained using the equation below and the results were expressed in mg/mL.

$$\frac{\text{Area of standard}}{\text{Area of the sample}} \text{ x } 20\ \mu g \Big/ \text{ml}$$

2.9.8. Qualitative analysis of phytochemicals from the extract of Helichrysum cymosum (Aqueous Q1 and ethanol Q2 extracts)

The phenolic contents of aqueous and ethanoic extracts of *H. cymosum* were determined by LC-SM analysis, which comprises a Waters Synapt G2 quadrupole time-of-flight mass spectrometer (MS) attached to the ultra-performance liquid chromatography (UPLC) (Waters, Milford, MA, USA) following the procedure reported by Idris et al. (2024) with slight modifications. ''Briefly, the ultra-performance liquid chromatography (UPLC) attached to the MS with 88 waters acquity and 89 was used for high-resolution UPLC-MS analysis. Electrospray ionization was used in negative 90 mode with a cone voltage of 15 V, desolvation temperature of 275 °C, a desolvation gas at 650 91 L/hr, and the rest of the MS settings optimized for best resolution and sensitivity''. Two (2 µL) samples were injected into the UPLC column, and the mobile phase composition consisted of solvent A (0.1% formic acid) and B (acetonitrile containing 0.1% formic acid) (Idris et al., 2024). The gradient for solvents alternated linearly from A at 100% for 1 min to 28% B in 22 min. Subsequently, it moved to 40% B in 50 s and a wash step for 1.5 min for 100% B, and then 40% B in 50 s and a wash step for 1.5 min for 100% B. It was equilibrated again to the initial conditions for 4 min. The following conditions were maintained for the column: flow rate: 102 0.3 mL/min, temperature: 55 °C. Ion mobility was set at IMS 104. The wave velocity was set at 332 m/s and the wave height at 20.2 V. Data were processed by scanning (from *m/z* 150 to 1500 in resolution mode as well as in MS^E mode). In the MS^E mode, the initial MS data was taken at a low collision energy (4 V), and the next one at a collision energy ramp (40–100 V). The reference mass (Leucine enkaphalin) was calibrated with sodium formate to obtain the appropriate mass measurements. Polyalanine was used for the 105 calibration and calculations.

Identification of compounds and designated names given was achieved through accurate mass matching using XCMS, which was connected to the following databases (MassBanks, Metlin, NIST, and ReSpect). All identified compounds were considered unidentified if the accurate mass match error (AME) was greater than 5 ppm (Zubarev and Makarov, 2013). The mass fragmentation patterns of compounds that were accessible were searched from these databases (Idris et al., 2023). The few phenolic compound standards that were spiked under similar LC-MS conditions and fragmentation patterns were identified based on retention time, mass fragmentation, and ionization mode (Okaiyeto et al., 2022a; Idris et al., 2023). Since UPLC-ESI-QTOF-MS could identify many compounds, therefore, all standards could not be obtained. Hence, information on MS and MS^2 fragmentation ions from the literature and databases was used to annotate these compounds. To minimize false annotations, the number of carbon atoms in the supposed identified compounds was estimated. Standard mixtures and chemical markers ranging from (3.9, 7.8, 15.6, 31.3, 62.5, 125.0, and 250.0 mg/L) were used for quantification. The calibration and linear curve were tested at the range of standard solution concentrations (mg/L) by plotting the peak areas against the standards and a correlation coefficient measured using linear regression, and an R-value greater than 0.99 was considered linear.

3. Statistical analysis

All results were evaluated by one-way analysis of variance (ANOVA), followed by a Bonferroni post-test using GraphPad Prism 5. Results were shown as a mean ± standard error of the mean, and statistical significance $P < 0.05$ was measured as substantial variation in the mean.

4. Results and discussion

Phytochemical contents present in plants are known for diverse medicinal healing potentials when applied (Al-Mustafa et al., 2021; Moriasi et al., 2021). Bioactive constituents of the genus *Helichrysum* have been well established as having anti-bacterial, antioxidant, anti-diabetic, anti-cancer, anti-inflammatory, and hepatoprotective potentials (Lourens et al., 2008; Lourens et al., 2011; Jadalla et al., 2022). The activities of this genus are linked to the occurrence of vital biomolecules such as flavonoids, phenolics, phloroglucinol derivatives, and others (Lourens et al., 2008). Furthermore, the species *H. cymosum* has been recently reported to have antidiabetic potential (Jadalla et al., 2022), antimalarial, antibacterial, and toxicity (Van Vuuren et al., 2006). In this research, the phytochemical constituents of *H. cymosum* were confirmed to contain secondary metabolites such as polyphenols and flavonols, which might be linked to the pharmacological potentials demonstrated by the plant. Thus, the current findings agree with other findings on this species (Akinyede et al., 2021b; Jadalla et al., 2022). Additionally, the findings revealed that the ethanol extracts had the greatest polyphenols and flavonols (303 ± 4 GAE/g, 183 ± 6 mg QE/g, respectively) compared to the aqueous extract (83.7 ± 2 GAE/g, 36.0 ± 1 mg QE/g, respectively), possibly because ethanol is a relatively much better extracting solvent for phenolic compounds (Al-Mustafa et al., 2021).

Antioxidant components in plants play a major role in modulating oxidative stress (OS)-induced complications (Benoite and Vigasini, 2021; Akinyede et al., 2021a; Akinyede et al., 2021b). Diabetic complications have been associated with OS as one of its fundamental causes, and this occurs when there is a buildup of free radicals, which are detrimental to human health, causing overproduction of mitochondrial superoxides, β-cell dysfunction, and diabetes vascular damage (Giacco

and Brownlee, 2010; Jadalla et al., 2022). Cell damage and mutation are known to be caused by free radicals, and natural antioxidant products are recognized to contribute significantly to clearing free radicals. Literature reports have shown that the inhibition of OS through antioxidants is essential in diabetes therapies, especially by protecting β-cell dysfunction in diabetes. Hence, the application of antioxidant-rich substances as therapeutic agents is plausible (Kifle and Enyew, 2020).

The current study investigated the in vitro antioxidant activities of *H. cymosum* AQ and ET extracts by assessing FRAP, TEAC (ABTS), and DPPH. The result demonstrated stronger antioxidant activity for the ethanol extract, and the highest effects were seen with DPPH (1893 ± 34 μmol TE/g), followed by FRAP (158 ± 2 μmol AEE/g), and then ABTS (1402 ± 26 μmol TE/g). Similarly, the antioxidant activities of the AQ extract were highest in DPPH (606 ± 8.4 μmol TE/g), followed by FRAP (530 ± 2 μmol AEE/g) and ABTS (450 ± 11 μmol TE/g). Thus, the DPPH, FRAP, and TEAC assays showed the strongest activities for the ET compared to the AQ.

The high antioxidant activity of the ET is surely linked to the presence of phytochemical constituents such as polyphenols and flavonols. Flavonoids, which are polyphenol and phenolic compounds, are known to possess potent antioxidant effects in mitigating the development of oxidative stress-related diseases. The phenolic antioxidant is known for interfering with the accumulation of ROS and other free radicals through the transfer of hydrogen atoms from its hydroxyl group, whereas the flavonoids are well established for their oxidative stability potentials by scavenging ROS and free radicals via oxidation, converting them to more stable and less reactive free radical forms (Akinyede et al., 2021a; Jadalla et al., 2022). Flavonoids are capable of reducing free radicals through quenching, chelating radical intermediate compounds, and upregulating or protecting antioxidant defense systems (Otang et al., 2012), and natural antioxidants can avert oxidative stress-related diseases such as diabetes (Benoite and Vigasini, 2021).

In general, the antioxidant activities exhibited by both AQ and ET extracts of *H. cymosum* could be linked to the reported phytochemicals they possess, displaying good scavenging activities. *H. cymosum* essential oils are known to have radical scavenging activities with a free radical scavenging concentration of SC_{50} = 6.3 g/l), in line with other studies (François et al., 2010). Additionally, an investigation by Adewinogo et al. (2022) presented the antioxidant potential of the essential oils of *H. cymosum* as having moderate antioxidant activities, in comparison to the current study, in which only the extracts exhibited strong antioxidant activities (Table 1).

4.1. High-Pressure liquid chromatography (HPLC) analysis

HPLC was used at 320 and 350 nm, respectively, for both the aqueous and 70% ethanol extracts, as shown in Figs. 1 (A and B) and 2 (A and B). Specific flavonoids were examined from both extracts, as shown in Table 2 below. The findings disclose compounds such as: caffeic acid (AQ), chlorogenic (AQ and ET), kaempferol (AQ), and rutin (ET). Further screening was then performed using UHPLC-ESI-MS (Figs. 3A and 3B) .

Table 1
Phytochemicals compound and antioxidant capacity of *H. cymosum* extracts.

Compounds/ antioxidant capacity	Aqueous extract	Ethanol extract
Polyphenols (mg GAE/g)	83.7 ± 2	303 ± 4
Flavonols (mg QE/g)	36.0 ± 1	183 ± 6
Flavanols (mg CE/g)	ND	ND
ABTS (μmol TE/g)	450 ± 11	1402 ± 26
FRAP (μmol AEE/g)	530 ± 2	158 ± 2
DPPH (μmol TE/g)	606 ± 8.4	1893 ± 34

All values are presented as mean ± SD (n = 3). GAE (gallic acid equivalent), AAE (ascorbic acid equivalent), TE (trolox equivalent), CE = Catechin equivalents, QE (quercetin equivalent), ND none detected.

4.2. Characterization of identified compounds isolated (UPLC) from *H. cymosum*

The ultra-performance liquid chromatograph (UPLC) was used to screen the phytochemicals present in the *H. cymosum* aqueous and 70% ethanol extracts, of which a total of 43 phytochemical derivatives were identified. These phytochemicals include hydoxycinnamic acids, flavan-3-ols, flavonol, helihumulone, and other compounds, as shown in Table 3.

4.2.1. Identification of hydroxycinnamic acids

Mono, di, and tri acyl chlorogenic acid were identified at peaks, 10–14, 22–26 and 27 respectively, presenting maximum absorption wavelengths at 300 and 326 nm of UV maxima (Idris et al., 2023). These spectra exhibited a deprotonated molecular ion at *m/z* 353 of mono caffeoyl quinic acids (mono-CQAs) and *m/z* 515 of di caffeoyl quinic acids (di-CQA). Fragmentation in the MS/MS produced *m/z* 191 (QA), which gave a dehydrated quinic acid moiety (*m/z* 173) and caffeic acid (*m/z* 179) as prominent fragments. The isomers were assigned using the hierarchical keys and order of elution sequence from the reversed-phase column previously developed as 3-O-caffeoylquinic acid (3-O-CQA) < 1-O-caffeoylquinic acid (1-O-CQA) < 5-O-caffeoylquinic acid (5-O-CQA) < 4-O-caffeoylquinic acid (4-O-CQA). Also, 4-O-CQA and 3-O-CQA were differentiated by the intensity of the characteristic ions of chlorogenic acids (Idris et al., 2023; Idris et al., 2024).

In the former, *m/z* 173 is the base peak, and in the latter, *m/z* 191 is the base peak (Crozier et al., 2009). Generally, CGAs with more hydroxyl groups in quinic tend to be more hydrophilic compared to those with more free axial hydroxyl groups. Meanwhile, the caffeoyl residue is easily removed in the course of fragmentation: 1 > 5 > 3 > 4 (Clifford et al., 2005). Given that hydroxyl groups are situated at the axial in positions 1 and 3, and the equatorial in positions 4 and 5 (Clifford et al., 2005; Idris et al., 2024), for di-O-CQAs, the more the additional caffeoyl groups are attached to free equatorial hydroxyl groups (owing to steric interactions), the stronger the retention (Clifford et al., 2005; Idris et al., 2024). Meaning, the loss of the caffeoyl group (C) is likely to be in the order of 1-C > 5-C > 4-C > 3-C (Clifford et al., 2005). This enabled peaks 22–26 to be classified as "1,3 di-O-CQA, 3,4 di-O-CQA, 1,5 di-O-CQA, 3, 5 di-O-CQA, and 4,5 di-O-CQA" respectively, since the elution order is "1,3-diCQA <<< 1,4-diCQA << 3,4-diCQA < 1,5-diCQA < 3,5-diCQA << 4,5-diCQA" (Clifford et al., 2005). The prominent ions for di-CQAs are 4,5-di-CQA, which has the base peaks *m/z* 353, 191, 179, and *m/z* 173, while 3,5-di-CQA has *m/z* 353 and 179 as base peaks (Schram et al., 2004). Di CQAs gave a maximum absorption wavelength of UV at 326 nm.

Earlier investigations on the chlorogenic profiling of *H. cymosum* revealed the presence of dicaffeoyl quinic acids from the acetonic extract (Matanzima, 2014). Peak 27 was identified as a tricaffeoylquinic acid using an accurate mass match, while Peak 5 was ambivalently recognized as p-Coumaric acid ethyl ester based on the presence of *m/z* 119 that would symbolize the decarboxylated coumaroyl. Additionally, a free dimethoxy cinnamic acid was allocated at peak 2.

4.2.2. Identification of flavan-3-ols

Many flavan-3-ols were in oligomeric/ or polymerized forms (peaks 18–21) and identified from the stereoisomers catechin and epicatechin. The monomers catechin, epicatechin, gallocatechin, and gallo(*epi*)catechin gave various lengths of polymers called proanthocyanidins (PAs). The two types of *B*-type PAs are linked by C4-C8 or C4-C6 interflavan linkages and *A*-type PAs have additional C2-C5 or C2-C7 interflavan ether-linkages, between the oligomers (Singh et al., 2018; Jimoh et al., 2024). The order of hydrophobicity for flavan-3-ol monomers in reversed-phase liquid chromatography, i.e. "(-/+)-epicatechin > (-/+)-catechin > (-/+)-epigallocatechin > (-/+)-gallocatechin," also enabled identification of the monomers and the oligoners (Jimoh et al., 2024). The order of elution from the column is in the opposite direction.

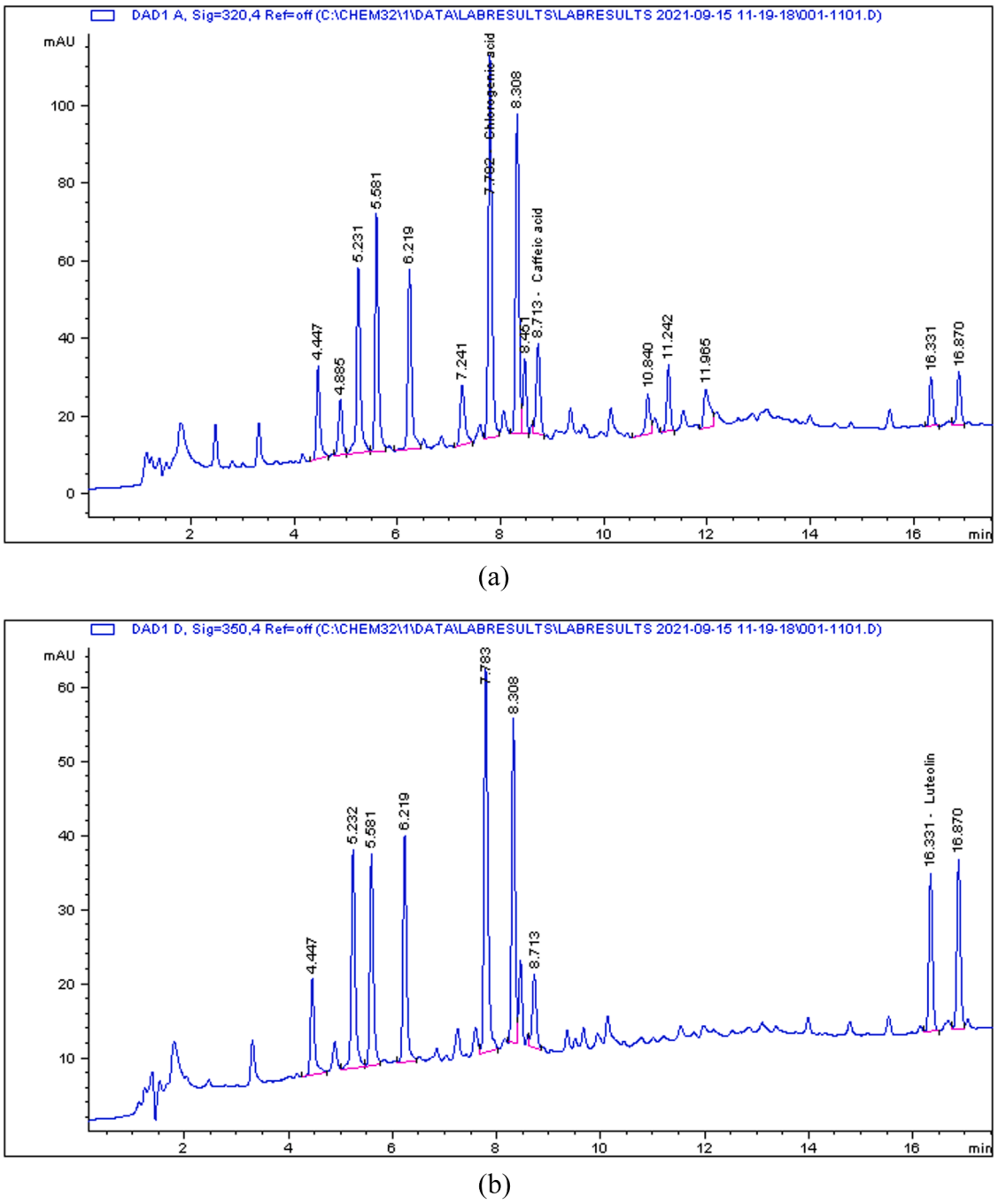

Fig. 1. HPLC chromatogram at 320 nm (A) and 350 nm (B) of aqueous extract of *H. cymosum*.

Thus, (-/+)-gallocatechin elutes earlier, and epicatechin comes out last. Diastereoisomers; "(–)-epicatechin (2R,3R) and (+)-catechin (2R,3S) resolve easily on reverse phase column packings, but (–)-epicatechin (2R,3R) and (+)-epicatechin (2S,3S), and (–)-catechin (2S,3R) and (+)-catechin (2R,3S)", do not (Clifford and Kuhnert, 2022).

Also, flavan-3-ols elute according to their degree of polymerization (DP), firstly eluting the monomers and then the different oligomers (López-Cobo et al., 2016). As reported by other authors, A-type procyanidins eluted before B-type procyanidins (Wallace and Giusti, 2010; López-Cobo et al., 2016; Gao et al., 2018). Catechin and epicatechin exhibit fragments *m/z* 151, 135 (due to retro Diels Alder (RDA) fragmentation) upon collision-induced dissociation (CID) of their precursor ions $[M-H]^{-;}$ *m/z* 289 (Idris et al., 2023; Jimoh et al., 2024). In addition, "fragment ions *m/z* 245 ([catechin-H-44]$^{-}$, loss of CO_2], *m/z* 205 [catechin -H-84]$^{-}$, loss of flavonoid A ring) and *m/z* 179 ([M-H-110]$^{-}$, loss of flavonoid B ring)" were consistent with that of literature (Escobar-Avello et al., 2019; Jimoh et al., 2024). Based on the above information, the assignment is indicated and represented in Table 3.

4.2.3. *Identification of flavonols*

Our study showed the presence of kaempferol and quercetin aglycones in confirmation with earlier reports (Matanzima, 2014), which was confirmed in this study at peaks 32–33 (Fig. 3B). However, some methylated and 6-methoxy quercetin derivatives of quercetin are being reported here for the first time. In addition, dihydrokaempferol has also been noticed at peak 34 (Fig. 3B), as previously reported in the literature for their MS/MS fragment ions (Dias et al., 2013).

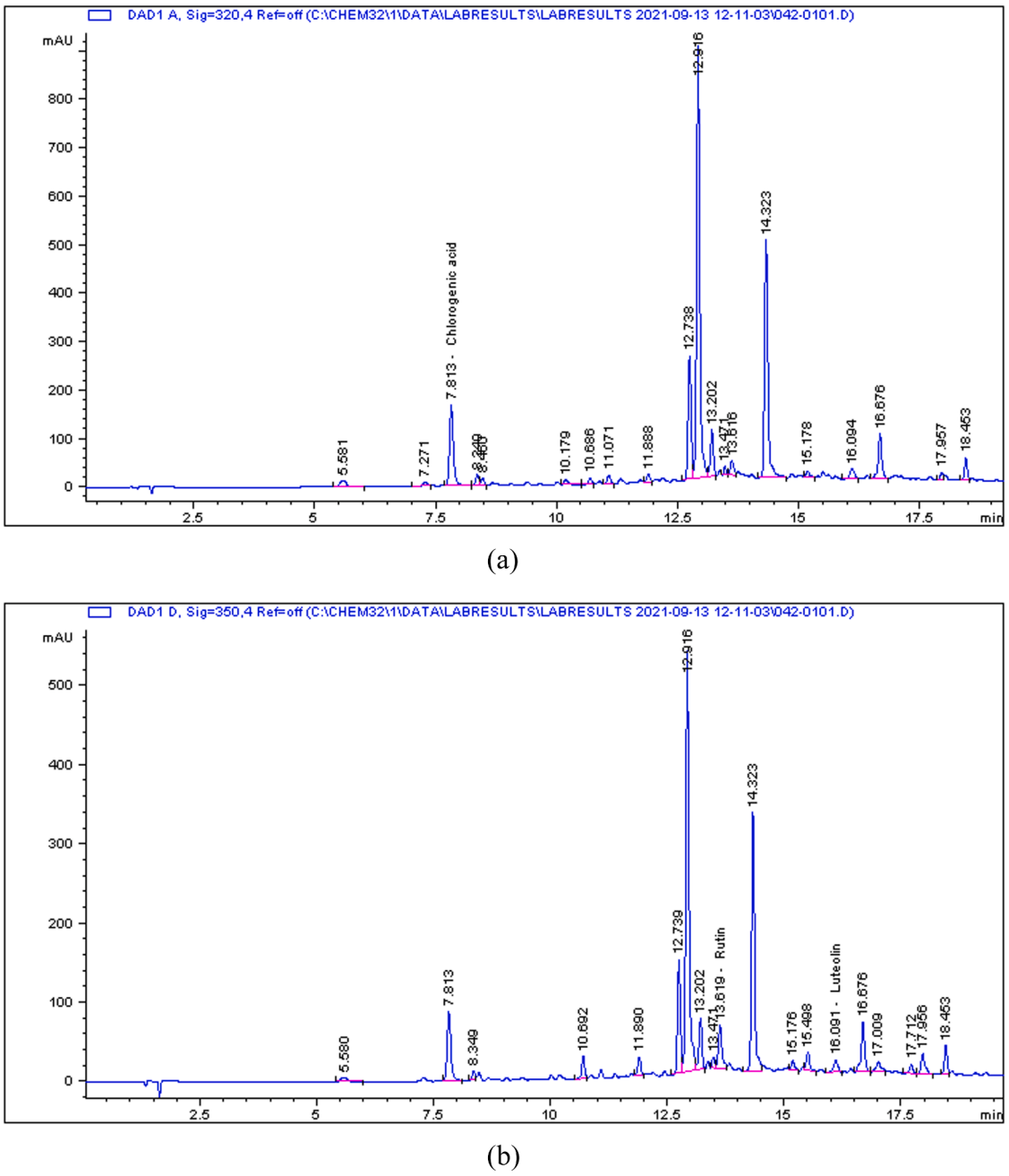

Fig. 2. HPLC chromatogram at 320 nm (A) and 350 nm (B) of 70% ethanol extract of *H. cymosum*.

Table 2
Phytochemicals compound of Aqueous and 70% ethanol extract of *H. cymosum* identified using high-pressure liquid chromatography (HPLC).

Compounds	unit	Aqueous extract	Ethanol extract
Caffeic acid	mg/g	0.28	0.00
Chlorogenic acid	mg/g	4.48	21.64
Kaempferol	mg/g	0.49	0.00
Rutin	mg/g	0.00	6.74

4.2.4. *Identification of other compounds*

Key among these compounds is helihumulone which has previously been isolated from the genus *Helichrysum* (Bohlmann et al., 1979; Matanzima, 2014) was reported with MS1 ion at *m/z* 423.0 and its high presence is indicated in this study (Fig. 3B). Some other compounds include carboxylic acids, piperic acid, malic acid, polyunsaturated fatty acids; oxo-dihydroxy-octadecenoic acid, and trihydroxy-octadecadienoic acid. Fragmentation of the carboxylic acids occurs through the release of one or two water (18 Da) and carbon dioxide (44 Da) molecules or both (62 Da), and is characterized by the ion fragments $[M - H\text{-}18]^-$and CO_2, $[M - H\text{-}44]^-$, or $[M - H\text{-}62]^-$ (Okaiyeto et al., 2022b; Idris et al., 2023). Amino acid at peak 9 was identified in negative ion modes as tryptophan, based on a deprotonated molecular ion peak $[M\text{-}H]^-$ at *m/z* 203.0 (Gouveia and Castilho, 2009). Additionally, its MS/MS spectrum displayed a fragment ion $[M\text{-}H\text{-}NH_3]^-$ at *m/z* 186. It is generally a fragmentation, generating the diagnostic 2-carboxy spiro[cyclopropane-indolium] fragment ion when ionized in positive mode.

4.3. *Evaluation of antidiabetic activities of aqueous and ethanol extracts*

4.3.1. *Alpha glucosidase inhibitory activity*

Alpha glucosidase are enzyme located in small intestines at the brush

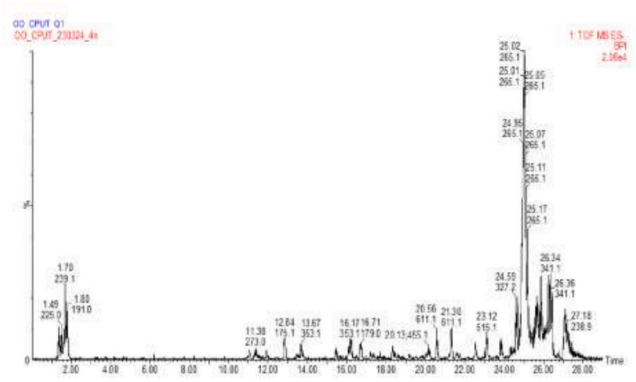

Fig. 3a. Shows UHPLC-ESI-MS base peak chromatogram for aqueous extract of *H. cymosum* analyzed in the negative ion mode.

border membrane of the enterocytes, where it breaks down dietary carbohydrates into monosaccharides for absorption. The enzymatic inhibition of alpha-glucosidase has been the main approach used in antidiabetic drug development since this enzyme is involved in carbohydrate metabolism to glucose (Kawamura-Konishi et al., 2012; Ghani, 2015; Visvanathan et al., 2021). Antidiabetic activities of most drugs and medicinal plants have been associated with the ability to inhibit enzyme activities (Oboh et al., 2014; Erukainure, 2018). In the present study, the alpha-glucosidase inhibitory activities by the aqueous (AQ) and ethanol (ET) extracts of *H. cymosum* was assessed and compared with acarbose (Fig. 4A). The results reveal significant inhibition by the aqueous extracts at lower concentrations (10 μg/mL and 50 μg/mL) while at 100 μg/mL AQ and the control, the same rate of inhibition with no significant ($p > 0.05$) difference was displayed. Equally, the ethanol extract showed maximum inhibition at (10 μg/mL) and at (50 μg/mL and100 μg/mL) with no significant ($p > 0.05$) difference compared to the standard drug acarbose. The current study revealed that the trend of alpha-glucosidase inhibitory activity is at its highest

Table 3
Phytochemicals screened from extract of *Helichrysum cymosum* (Aqueous Q1 and Ethanol Q2 extracts) using LCMS.

Peak	t_R (min)	UV λ_{max} (nm)	*m/z* [M-H]$^-$	MS/MS	Tentative name	Sample	Identification
1	1.39		248.9	181, 1	Piperic acid	Q1, Q2	Jimoh et al. (2024)
2	1.49		225.0	179, 215	Dimethoxycinnamic acid monohydrate	Q1, Q2	Idris et al. (2024)
3	1.62		317.0	215, 165, 195, 174	Benzoyl galactonic acid Derivative	Q2	New
4	1.70		239.1	229, 207, 193	Flavonol	Q1, Q2	Idris et al. (2024)
5	1.80		191.0	149, 119	p-Coumaric acid ethyl ester	Q1, Q2	Akinyede et al. (2022)
6	1.88		133.0	133, 7	Malic acid	Q2	Abd Ghafar et al. (2020)
7	11.38		272.9	175, 192	Esculetin derivative	Q2	Idris et al. (2024)
8	12.84		175.1	145	Esculetin	Q1, Q2	Idris et al. (2024)
9	13.47		203.1	185, 2	L-Tryptophane	Q2	Soto Mayer (2019)
10	13.67	323	353.1	179, 135, 191	3-caffeoylquinic acid	Q1, Q2	Yang et al. (2022)
11	16.09	326 sh	353.1	191, 173	1-caffeoylquinic acid	Q2	Yang et al. (2022)
12	16.17	326	353.1	191, 179	5-caffeoylquinic acid	Q1, Q2	Akinyede et al. (2022)
13	16.24	325	353.1	179	4-caffeoylquinic acid	Q2	Idris et al. (2023)
14	16.71	322	179.0	135	Caffeic acid	Q1	Akinyede et al. (2022), Idris et al. (2023)
15	18.39	373	565.1	519, 169	Galloyl derivative	Q2, Q1	Idris et al. (2024)
16	19.02		423.1	unfragmented	Helihumulone	Q2	Matanzima (2014)
17	20.13	266	455.1	173, 225	O-Methylated (+)-Catechin gallate	Q1	Nešović et al. (2020)
18	20.56	280	611.1	457, 367, 225	(+)-gallocatechin-3-Ogallate -derivative	Q1	Alperth et al. (2019)
19	20.61	280	611.1	575, 197, 357	(-/+)- gallocatechin-derivative	Q2	Abu-Reidah et al. (2014) Alperth et al. (2019)
20	21.32	282	609.1	197	(-/+)-(Epi)gallocatechin-(*epi*) gallocatechin	Q1, Q2	Alperth et al. (2019)
21	21.39	341	611.1	575, 4	(-/-)-(Epi)gallocatechin-(*epi*) gallocatechin	Q2	Alperth et al. (2019)
22	22.62	325	515.1	353, 173, 179, 191	1,3- Dicaffeoylquinic acid	Q2	Yang et al. (2022)
23	23.13	327	515.1	191, 353, 179, 135	3,4-Dicaffeoylquinic acid	Q2	Yang et al. (2022)
24	23.18	327 sh	515.1	353, 179, 191	1,5- Dicaffeoylquinic acid	Q2	Yang et al. (2022), Idris et al. (2023)
25	24.09	327 sh	515.1	353, 173, 179, 191, 135	3,5- Dicaffeoylquinic acid	Q2	Akinyede et al. (2022), Yang et al. (2022); Idris et al. (2023)
26	24.11		515.1	353	4,5- Dicaffeoylquinic acid	Q2	Yang et al. (2022)
27	24.37	293, 327	677.1	467, 5	3,4,5-Ttricaffeoylquinic acid		Yang et al. (2022)
28	24.47	340	681.2	331, 3	6-methoxyquercetin derivative	Q2	Idris et al. (2024)
29	24.53	341	315.0	300, 271, 255	O-Methyl quercetin		Mohamed et al. (2024)
30	24.59	289	327.2	215, 265, 293	oxo-dihydroxy-octadecenoic acid	Q1	Idris et al. (2023), Idris et al. (2024); Jimoh et al. (2024)
31	24.67	295	329.2	265, 293, 227, 129	Trihydroxy-octadecadienoic acid	Q1	Idris et al. (2024), Jimoh et al. (2024)
32	24.83		299.1	255	Quercetin	Q2	Matanzima (2014)
33	24.89	340	285.1	255, 265	Kaempferol	Q2	Matanzima (2014)
34	24.92	289, 335	287.1	255, 265, 255, 269	Dihydrokaempferol	Q2	Idris et al. (2024)
35	25.01	280, 330	265.1	149	Magnolol	Q2	Li et al. (2023, Jimoh et al. (2024)
36	25.02	287	265.1/ 293.2	150	2′-Deoxyguanosine monohydrate	Q1	New
37	25.17	283	265.1	150	Magnolol	Q1, Q2	Li et al. (2023, Jimoh et al. (2024)
38	25.87	280, 323	423.2	279			
39	26.34		341.1	150, 265, 293, 279	Magnolol derivative	Q1, Q2	Li et al. (2023), Jimoh et al. (2024)
40	26.36		461.2	379, 341, 265, 150, 249	Pentoside derivative	Q2	New
41	26.43		341.1	150	Not identified	Q2	New
42	26.56		341.1	157	Not identified	Q2	New
43	27.20		238.8	239	Not identified	Q1, Q2	New

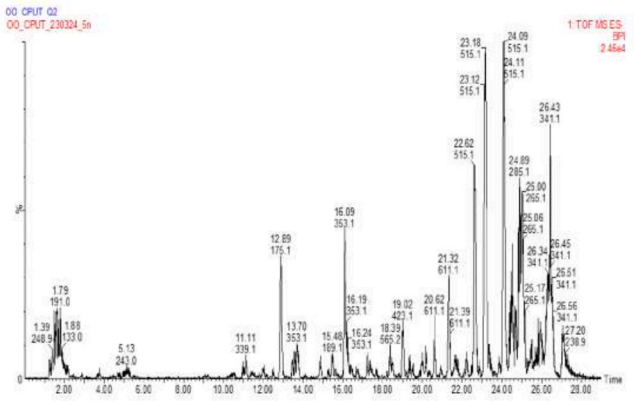

Fig. 3b. Shows UHPLC-ESI-MS base peak chromatogram for 70% ethanol extract of *H. cymosum* analyzed in the negative ion mode.

potential at lower concentrations and declines steadily with increased concentrations. The lowest inhibition was observed at 250 μg/mL, 500 μg/mL, and 1000 μg/mL, respectively compared to acarbose**.** The finding suggests that *H. cymosum* contains phytochemical such as flavonoid and polyphenols which have a strong affinity to the enzyme binding site better at lower concentration that higher concentration (Ramkumar et al., 2010; Proença et al., 2022). The lower inhibitory effect at higher concentration could be attributed to saturation of the enzyme active site by the compounds or binding to other areas of the enzyme rather than the active side by lowering it inhibitory effects. Another potential factor might be due to competitive inhibition, where both compound and substrates contend for occupancy of the enzyme active site, thereby affecting their enzyme binding affinity (Proença et al., 2022). Nevertheless, the alpha-glucosidase inhibition presented in this study can be linked to the presence of the following compounds; quercetin, chlorogenic acid, catechin and its derivatives, caffeic acid, kaempferol and which have also been reported in other studies to be an effective alpha-glucosidase inhibitors (Lin et al., 2016; Tian et al., 2016; Erukainure, 2018; Pimpley et al., 2020). The observed, hypoglycemic effect displayed by *H. cymosum* extracts, accords to earlier investigation by Jadalla et al. (2022) in which *H. cymosum* methanoic extract exhibited strong alpha-glucosidase inhibitory activity with IC_{50} value of 12.94 ± 0.2 μM 18.16 ± 1.2 and 44.44 ± 0.2 μM respectively. Enzymatic inhibition of alpha-glucosidase by *H.cymosum* portrays a potent hypoglycemic agent that can be used to regulate the amount of blood glucose by limiting glucose absorption into the blood stream (Erukainure, 2018).

4.3.2. *Alpha amylase inhibitory activity*

Alpha amylase is a digestive enzyme that enables the breakdown of polysaccharides into glucose and maltose (Kaur et al., 2021). The alpha-amylase inhibitory activities of aqueous and ethanol extracts of *H. cymosum* at various concentrations is shown in Fig. 4B. The results show that there was substantial inhibition of alpha-amylase at the lowest concentration (10 μg/mL) for both aqueous and ethanol extracts,

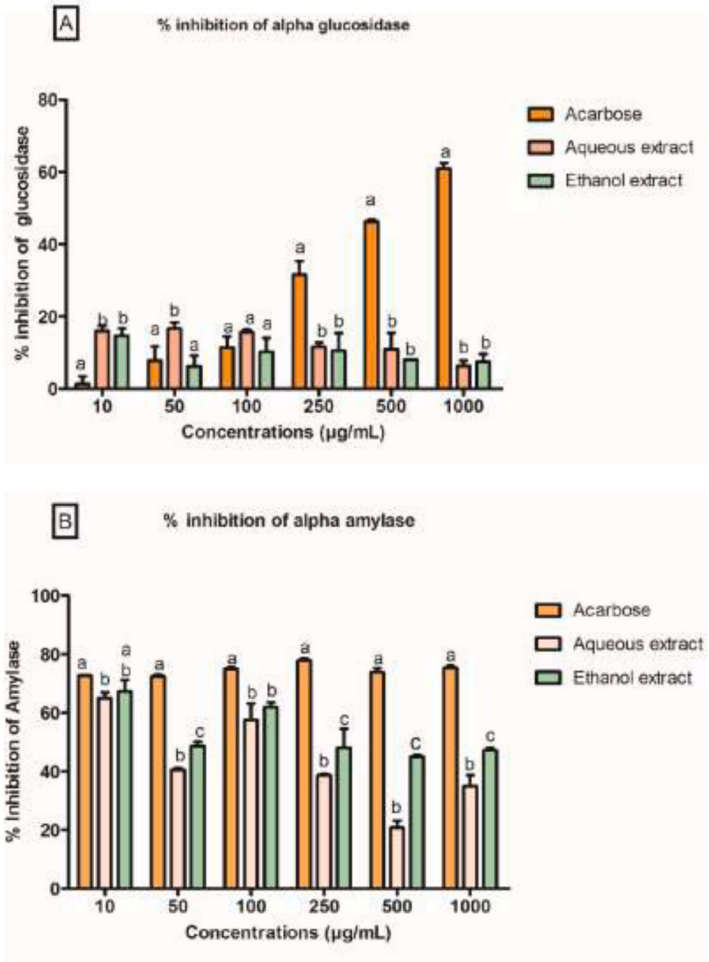

Fig. 4. α-glucosidase (A) and α-amylase (B) inhibitory activities of aqueous and 70% ethanol extracts of *Helichrysum cymosum*. Data were express as mean ± SD; $n = 3$. The bars with different letters shows significantly different ($p < 0.05$). The % inhibition was compared to the control acarbose.

approximate to that of the control (acarbose), while the other concentrations show moderate activities, but the efficacy was lesser than that of acarbose. Earlier study by Jadalla et al. (2022) reported no measurable alpha-amylase inhibitory activity of *H. cymosum* methanoic extracts. Therefore, the lower activity exhibited by both extracts in this study could be ascribed to the minimal interaction and binding affinity of the phytochemical constituents with alpha-amylase (Lu et al., 2017; Kaur et al., 2021). Perhaps, the different compound present in *H. cymosum* were engaged in a competitive mode with the substrate for same binding site of the enzymes, thus preventing the action of the compound in inhibiting alpha amylase enzyme (Zhang et al., 2015). Inhibition of carbohydrate- hydrolyzing enzyme activities by compound such phenolic is based on their ability to bind with proteins. Phenolic compounds such as flavonoids and phenolic acid have been associated with antidiabetic activities via enzyme inhibition (Agarwal and Gupta, 2016). Other bioactive compounds such as anthocyanins, carotenoids, flavonoids, phenolic, and vitamins have equally been reported to inhibit α-amylase in diabetic patients, by preventing the mechanisms that are involved in the development of diabetes (Agarwal and Gupta, 2016).

4.3.3. Pancreatic lipase inhibition

The pancreatic lipase inhibitory activity of *H. cymosum* aqueous and ethanol extracts is shown in (Fig. 5). The findings show a lesser and significant ($p < 0.05$) inhibitory effect on lipase enzyme at all concentration for both extracts compared to the standard drug orlistat (control), suggesting that the biomolecule present in *H. cymosum* might have very low affinity for pancreatic lipase enzyme binding site, thus hindering it effectiveness (Li et al., 2021). Similarly, a study by Pringle et al. (2021) showed that *A. linearis* has no inhibitory effects on pancreatic lipase. Despite the diminished effect of *H. cymosum* extracts toward pancreatic lipase enzyme, the bioactive compound could still exert its therapeutic effect in combating obesity and hypertriglyceridemia in type 2 diabetes via other mechanistic pathways such as AMPk-activated protein kinase, PI3K, phosphatidylinositol 3-kinases; AKT, protein kinase (Lv et al., 2019; Savova et al., 2023; Nethengwe et al., 2024). Therefore, the importance of extracts' action through these pathways PI3K/AKT/ AMP, cannot be omitted, they could have a downstream effect on insulin action and activation of different organs like adipose tissue, liver and muscle. Studies have shown that activation of these signaling pathways PI3K/AKT/ AMPk /GSK3 have antidiabetic and lipid modulatory effect by the extract of *Hypericum attenuatum* Choisy in mice (Lv et al., 2019). The findings suggest that antidiabetic modulatory effect H. *cymosum* extracts is more dominant toward carbohydrate metabolizing enzymes with a less impact on triglycerides. However, the adipogenic approach could be the potential mechanism via which the extracts could potentially modulate obesity (Savova et al., 2023).

4.3.4. Cytotoxicity assays (MTT)

The cytotoxicity effect of aqueous (AQ) and ethanol (ET) extracts were examined on C3A hepatocyte using melphalan as positive control. Cells were treated with AQ and ET extracts at various concentrations (7.8 μg/mL; 15.6 μg/mL; 31.25 μg/mL; 62.5 μg/mL; 125 μg/mL and 250 μg/mL) for 48 h. The AQ extracts (Fig. 6A) did not show any significant difference ($p > 0.05$) in cell viability at all concentrations compared to the untreated control, however, there was a significant increase ($p < 0.05$) by *H. cymosum* AQ extracts at all concentration compared to the melphalan treated control. From this finding, it was observed that the AQ extracts gradually increase cell viability at lower concentrations up till (7.8 μg/mL; 15.6 μg/mL; 31.25 μg/mL) and then slowly decreases at higher concentrations (62.5 μg/mL; 125 μg/mL and 250 μg/mL), suggesting that *H. cymosum* AQ extracts gradually enhanced cell viability to a certain ranges of concentration and then start to induce cellular stress on cells, hence decrease in cell proliferation, although there was no significant difference ($p > 0.05$) compared to the untreated control. The results demonstrated the safe use of AQ extracts at all concentrations. The ET extract (Fig. 6B) exhibited a significant ($p < 0.05$) increase in cell proliferation from (7.8 μg/mL; 15.6 μg/mL; 31.25 μg/mL; 62.5 μg/mL; 125 μg/mL) compared to melphalan treated control and no significant change ($p > 0.05$) with 250 μg/mL concentration. When compared to the untreated controls, the ET extracts of *H. cymosum* showed no significant difference from the lowest concentration up to 125 μg/mL but at 250 μg/mL, there was a significant decreased cell viability, which was indicative of toxicity ($p < 0.05$). The findings indicate that the ET extracts is safe for use at lower concentrations, whereas higher concentration pose a toxicity threat and requires careful evaluation.

4.3.5. Anti-inflammatory activities and cellular antioxidant activities

The mouse macrophage cell line, RAW 264.7, is a well-characterized and popular model to investigate the anti-inflammatory potential of test samples. Cells were cultured in multi-well plates and activated by exposure to LPS which induces the expression of iNOS with concomitant nitric oxide formation. Changes in NO production were determined by measuring the levels of nitrite in the culture medium. Simultaneous evaluation of cell viability (MTT assay) was used to confirm the absence of cytotoxicity in the test sample. The current study adopted this model to evaluate the anti-inflammatory potentials of *H. cymosum* aqueous and 70% ethanol extracts. The observed anti-inflammatory activity as shown in Fig. 7 (A–D) indicated a decrease in nitrite concentration in response to LPS activation of RAW macrophages with no effect on cell viability ($p > 0.05$), as seen with the AG-treated cells. The AQ treated cell shows a higher NO production at all concentrations with no effect on cell viability ($p > 0.05$) (Fig. 7 E and F). The AQ treated cells showed no significant ($p > 0.05$) inhibition of NO compared to LPS treated cells and its cell viability, whereas control and the AG treated showed a significant ($p < 0.05$) reduction in NO with no effect on cell viability (Fig. 7 A, B, C, and D) .

The ethanol extract (Fig. 7 B) exhibited a slight decrease in NO production at 50 μg/mL ($p < 0.05$) compared to LPS treated cells and could possess anti-inflammatory potential, however, the ethanol extract showed cytotoxicity at concentrations of 100 and 200 μg/mL with

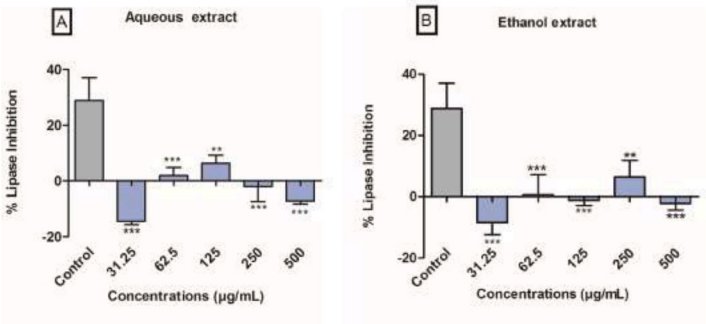

Fig. 5. Pancreatic lipase inhibition of aqueous (A) and 70 % ethanol (B) extracts *of H. cymosum*. Error bars indicate the standard deviation of the mean of four replicates. The * on the bars indicate significant difference ($p < 0.05$) compare to the control orlistat (100 μM).

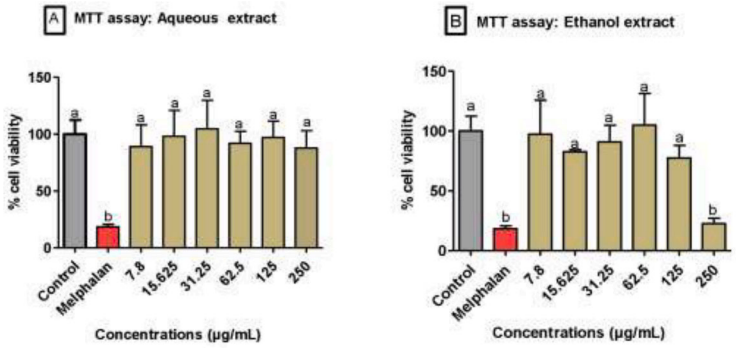

Fig. 6. Cytotoxicity evaluation of aqueous (A) and 70% ethanol (B) extracts of *H. cymosum* against C3A cells after 48 h. Melphalan was used as positive control. Error bars indicate standard deviation of mean four replicate. Bars with different letters present significant different ($p < 0.05$) compared to the untreated control.

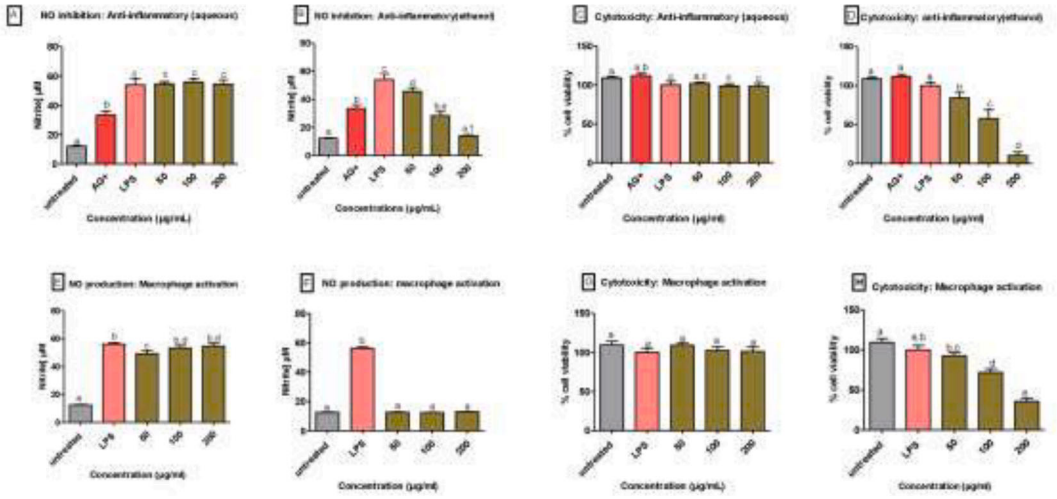

Fig. 7. Nitric oxide production and inhibition of LPS-activated macrophages (A, B, E, and F), and their corresponding cell viability (%) (C, D, G, and H) after 24 h treatments with aqueous and 70 % ethanol. Error bars indicate standard deviation of mean four replicate. Bars with different letters present significant different ($p < 0.05$) compared to the AG- control and untreated control.

significant ($p < 0.05$) inhibition of NO, but the results of these concentration cannot be considered (Fig. 7 B and D) . Similarly, macrophage activation was indicated by a significant ($p < 0.05$) reduction in NO production with significant decline in cell viability for the ethanol treated cells (Fig. 7 F and H) . It could be said that the ethanol extracts possess anti-inflammatory effect at minimal concentrations but toxicity concerns for higher concentrations. For the aqueous extracts, the ineffectiveness on NO inhibition, despite maintaining cell viability does not roll out its potency toward inflammatory responses, it action could be of importance via other anti-inflammatory inhibitory channel or routes such as cytokines production (Nemudzivhadi and Masoko, 2014).

Oxidative stress and inflammatory response have been associated with the accumulation or buildup of free radicals (Diaz et al., 2012; Nemudzivhadi and Masoko, 2014). Reactive oxygen species (ROS) have been implicated in mediating cytokine productions through the activation of transcription factors like NF − κB, indicating that there is a connection between ROS and cytokines to initiate an inflammatory response (Nemudzivhadi and Masoko, 2014). However, the inflammatory response is well known to be a protective mechanism against ailments, but on the flip side, unending inflammatory actions could result in tissue dysfunction (Ravipati et al., 2012; Nemudzivhadi and Masoko, 2014; Okaiyeto et al., 2022a). Additionally, excess accumulation of free radicals can interact with pro-inflammatory molecules resulting in the production of superoxides and peroxynitrites which can cause permanent cell membrane damage (Ravipati et al., 2012). Previous studies have uncovered natural anti-inflammatory compounds such as phenolic and flavonoids to play an important role as anti-inflammatory agents (Diaz et al., 2012; Ravipati et al., 2012; Wen et al., 2015). The anti-inflammatory effects shown by the ethanol extract is suggestive of the presence of phenolic compounds.

Therefore, interfering with the production of ROS by natural antioxidants is an effective strategy to overcome and prevent OS and its subsequent damage to organs (Palomino et al., 2022).

4.3.6. *Cellular antioxidant activities*

Cellular antioxidant activity (CAA) is used to quantify the antioxidant capacity of bioactive compounds or phytochemicals in cells, using an oxidant in conjunction with a fluorescent probe specific for the detection of reactive oxygen species (ROS) (Wolfe and Liu, 2007; Wen et al., 2015). This approach provides knowledge by considering the antioxidant behaviors, uptake distribution, and metabolism in physiological conditions (Wen et al., 2015). In the current study, CAA analysis was used to determine the antioxidant activities of *H. cymosum* aqueous and ethanol extracts in C3A hepatocytes using (TBHP) and the CellROX® Orange reagent (Molecular Probes®, Life Technologies, USA). TBHP, a short-chain organic hydroperoxide, is commonly used to induce cellular oxidative stress as its metabolism results in the production of peroxyl and alkoxyl radicals (Yang et al., 2020). CellROX® Orange is a cell-permeable, reduced, non-fluorescent dye that becomes brightly fluorescent upon oxidation by ROS, with excitation/emission maxima of 640/665 nm, respectively. The observed activity reflects both the direct ROS scavenging activity of the samples, as well as any potential changes

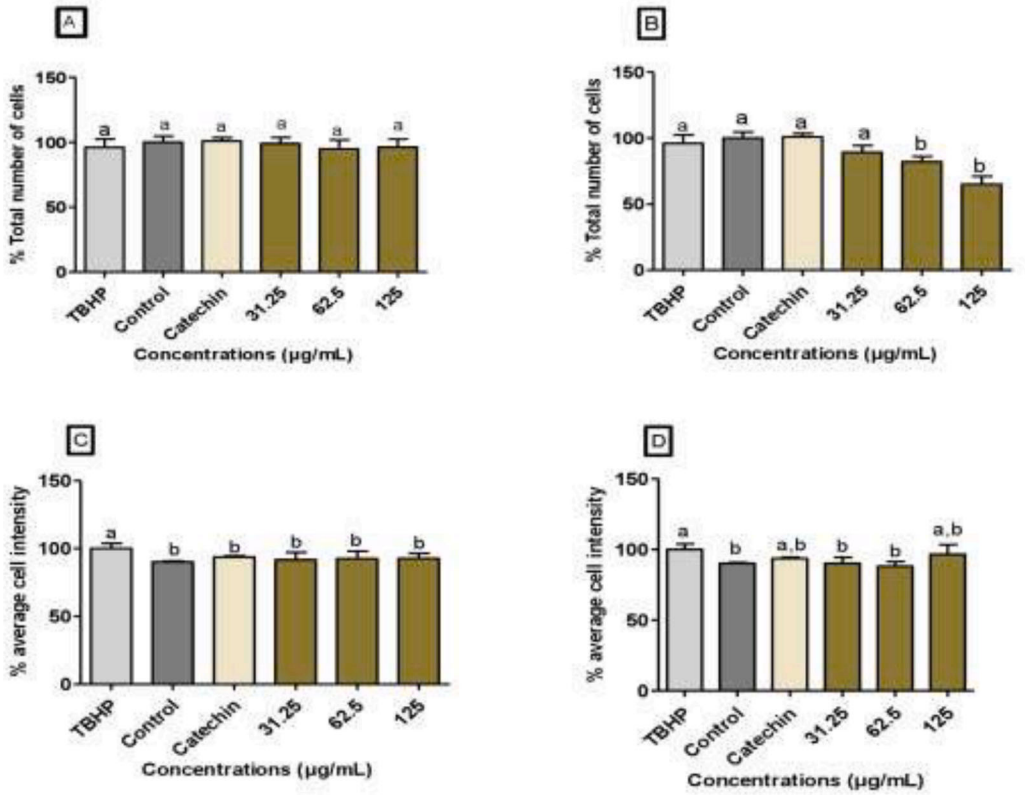

Fig. 8. Cellular antioxidant activity of C3A cells: Total number of cells (%) (A and B) and Average Intensity (C and D), after 24 h of treatment with aqueous (A and C) and 70 % ethanol (B and D). Catechin (100 µM) was used as a positive control and significant toxicity ($p < 0.05$ compared to TBHP). Error bars indicate standard deviation of quadruplicate values obtained from a single experiment. Different letters above the bar for each given concentration compared to the control are significantly different ($p < 0.05$).

in the inherent capacity of the cells to resist oxidative stress as cells are pre-treated with aqueous and ethanol extracts for 24 h before exposure to TBHP (Martín et al., 2001; Singh et al., 2018; Norfaizah, 2020).

The cellular antioxidant activity of aqueous and ethanol extracts was determined in C3A cells using TBHP as an oxidant and CellROX® Orange as a quantitative indicator of ROS. Catechin (100 µM) was used as a positive control to indicate antioxidant activity as shown in Fig. 8(A and B), indicating that the aqueous extract was not cytotoxic at all concentrations, whereas significant cytotoxicity was observed in C3A hepatocytes after treatment with the ethanol extract (62.5 and 125 µg/mL), hence, their antioxidant capacity at those concentrations cannot be reliably interpreted. On the other hand, the aqueous extract exhibited antioxidant activity at a treatment concentration of 31.25 and 125 µg/mL. Although the reduction at 62.4 µg/mL was not statistically significant, the ethanol extract showed significant inhibition of TBHP-induced ROS production at 31.25 and 62.5 µg/ml.

One previous study has shown that dietary antioxidants could as well act as pro-oxidants in cell culture systems and might result to cellular damage (Martin et al., 2008), thus the variation of antioxidant activities of the different doses in the current study suggest that higher concentrations of test sample can enhance oxidative stress damages. However, ethanol extracts were cytotoxic at these concentrations (62.5 and 125 µg/mL) after 24 h treatment. The cytotoxic effect observed by the ethanol extract at these concentrations could be attributed to the identified phytochemical compounds such as flavonoids (Olabiyi et al., 2020; Okaiyeto et al., 2022b). These compounds may disrupt of the trans-membrane protein flux, hence inhibiting cell proliferation (Sohn et al., 2013).

Previous studies showed that assessing the ROS produced directly in living cells is a pointer to oxidative damage. The pro-oxidant TBHP, a short-chain organic hydroperoxide, is commonly used to induce cellular oxidative stress as its metabolism results in the production of peroxyl and alkoxyl radicals (Martín et al., 2001; MARTin et al., 2008). It was observed that the ROS produced in cultured cells during this study was reduced significantly at all ranges of concentrations with the aqueous extracts and at lower concentrations for ethanol extract. This reveals that the natural antioxidants present in *H. cymosum* could reduce the generation of ROS in the C3A cell lines, thereby preventing oxidative stress damage to cells. Thus, the quenching of ROS by the *H. cymosum* extracts could improve oxidative stress damage. The aqueous extract showed promising activities at all tested concentrations, while the effects of the ethanol extract were seen at lower concentrations. Thus, lower concentrations of ethanol should be considered for use in future studies.

4.3.7. Glucose uptake and utilization in C3A hepatocytes and L6 myocyte cell

Glucose uptake and its utilisation are important regulatory pathways used in the clearance of glucose in the bloodstream in normalising blood glucose levels (Chadt and Al-Hasani, 2020). Fig. 9.1 (A–D) shows glucose utilisation by C3A hepatocytes after 24- and 48-hour treatment with aqueous and ethanol extracts. The AQ 24 h treatment demonstrated progressive increase in glucose utilization from lowest to the highest in a concentration-dependent order compared to the untreated control, a significant increase ($p < 0.05$) was noted at higher concentrations (30, 60, and 120 µg/mL) (Fig. 9.1A). Meanwhile the 48 h AQ treatments showed a minor and insignificant increase across all concentrations compared to the control ($p > 0.05$) (Fig.9.1C), Also cell viability was >70% across all concentrations, therefore, no toxicity was recorded.

ET (24 h) shows continuous increase in glucose utilization across all concentrations, a higher and significant ($p < 0.05$) glucose utilization was attained at 15 and 30 µg/mL, with no toxicity, whereas toxicity was

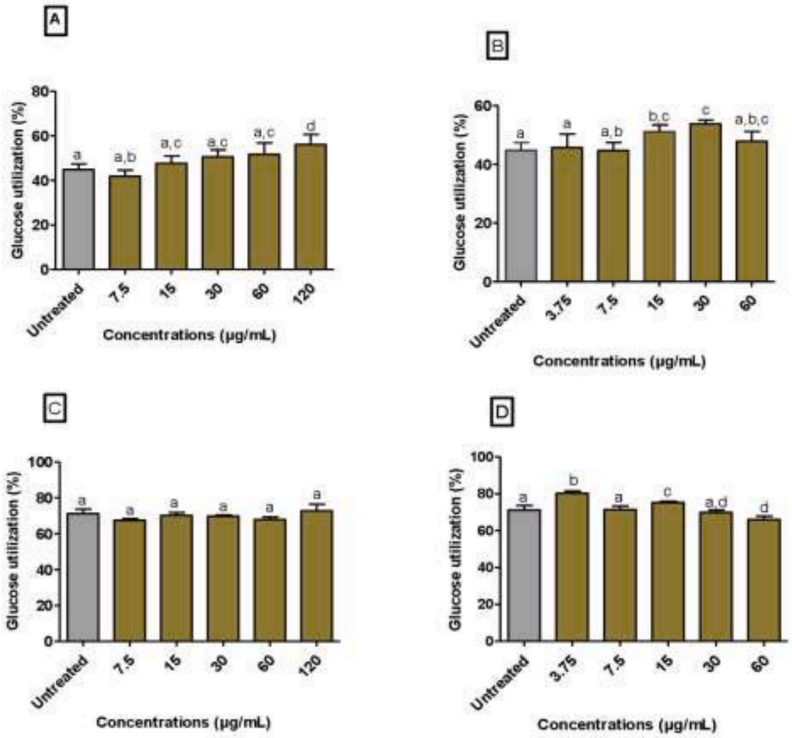

Fig. 9.1. Glucose utilization (%) after 24 h (A and B) and 48 h (C and D) of treatment by *H. cymosum* in C3A hepatocytes. Results were normalized to cell viability as determined using the MTT assay. Error bars indicate the standard deviation of the mean of four replicates. Letter above the bars indicates a significant difference ($p < 0.05$) compared to the control.

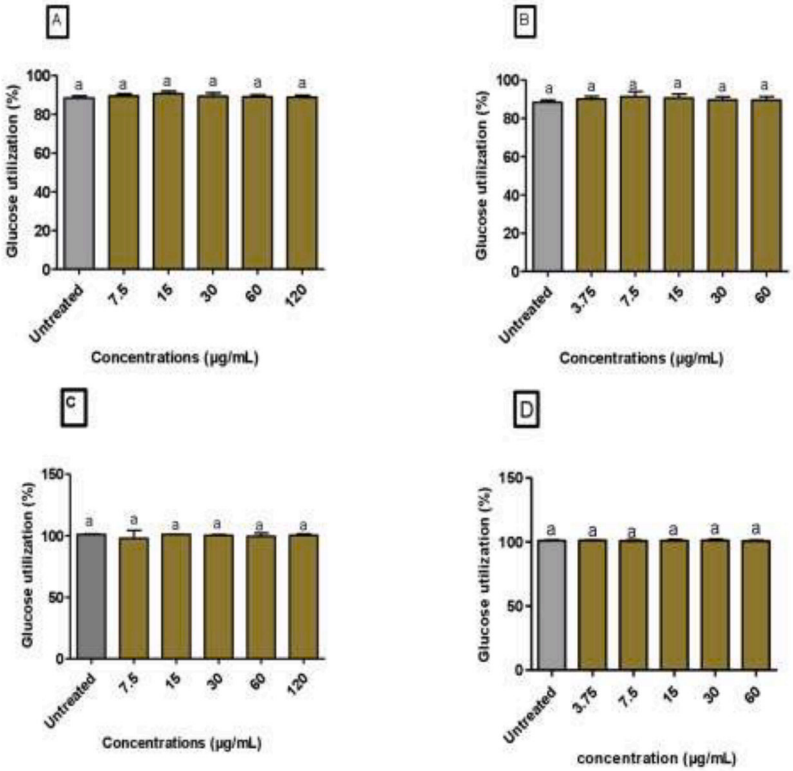

Fig. 9.2. Glucose utilization (%) after 24 h (A and B) and 48 h (C and D) of treatment by *H. cymosum* in L6 myocytes cells. Results were normalized to cell viability as determined using the MTT assay. Error bars indicate the standard deviation of the mean of four replicates. Letter above the bars indicates a significant difference ($p < 0.05$) compared to the control.

observed at 60 μg/mL compared to the control (Fig. 9.1B), whereas, for the ET 48 h treatment, the highest glucose utilization was attained at lower 3.75 μg/mL and 15 μg/mL ($p < 0.05$) and toxicity was exhibited at the highest concentration (30 and 60 μg/mL) (Fig. 9.1D). The glucose utilization for L6 myocyte cells after 48 h for both AQ and ET shows that the cells utilized all the available glucose (Fig. 9.2C and D). For the 24 h glucose utilization in a L6 myocyte cells, a very small substantial increase was observed after normalizing with MTT cell viability although statistically insignificant ($p < 0.05$) at 15 μg/mL for AQ and 0.7, 7.5 and 15 μg/mL for ET (Fig. 9.2A and B, respectively)

Glucose uptake in L6 Myocyte cells shown in Fig. 9.3 (A–D) demonstrated a significant increase in glucose uptake at 15, 30, and 60 μg/mL (Fig. 9.3A) and 7.5, 15 and 30 μg/mL for (Fig. 9.3B) after 24 h compared to control ($p < 0.05$) and no significant difference ($p > 0.05$) compared to Insulin. After 48 h treatment, samples show no significant increase compared to the control (Fig. 9.3 C and D) , no toxicity was recorded, and cell viability was >70% at all concentrations. Glucose uptake by C3A hepatocyte cells within 48 h of treatment as shown in Fig. 9.3 (F and G), demonstrated a comparable glucose uptake to that of the control within all concentrations for AQ (Fig. 9.3F). Likewise, ET (Fig. 9.3 G) exhibited similar rate in glucose uptake across the various concentrations except at 7.5 μg/mL which had a slight decline compared to the untreated control, while insulin had a higher glucose uptake compared to all concentrations in both AQ and ET extracts. The observed glucose uptake and its utilization by C3A and L6 myocytes could have been enhanced by bioactive phytochemical constituent of *H. cymosum*. The findings reveal that the phenolic compound present in H. *cymosum*, could potentially modulate glucose metabolism by influencing cellular uptake in glucose responsive cells (muscle and fat), by enhancing its glucose uptake and utilization (Abifarin et al., 2021; Olaokun et al., 2017).

Studies have established the important role played by glucose transporter in the distribution of glucose via cell surface membrane to storage organs (muscles and adipose tissues) and in maintaining normal blood glucose levels (Okaiyeto et al., 2022b). However, GLUT4 remains the most projected among other GLUTs for insulin regulation and glucose transport in adipose and skeletal muscles (Pereira et al., 2017; Chadt and Al-Hasani, 2020). GLUT4 facilitates glucose uptake via insulin action which stimulates the transportation of GLUT4 proteins across the plasma membrane (Satoh, 2014; Sayem et al., 2018; Joost et al., 2002; Leto and Saltiel, 2012). Insulin promotes glucose uptake by increasing the concentration of Glut4 protein at the plasma membrane

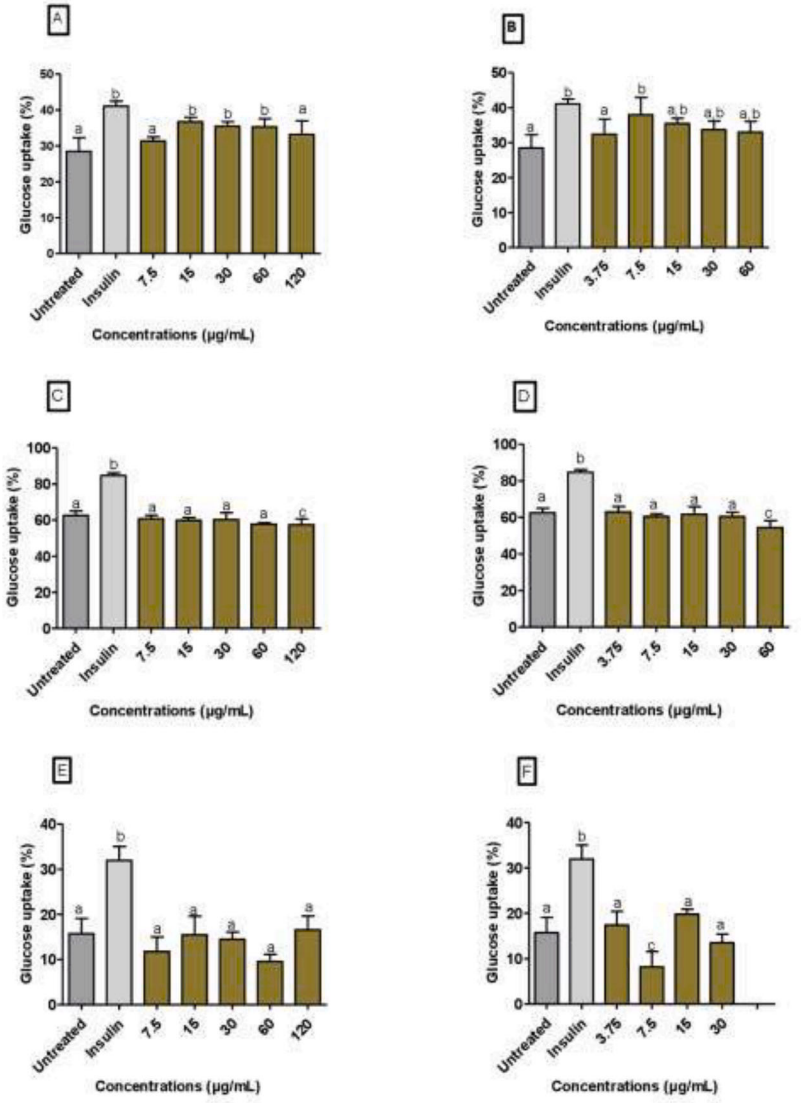

Fig. 9.3. Glucose uptake (%) by L6 myocytes and in C3A hepatocytes, following 48-hour pre-treatment with H. cymosum aqueous and ethanol extracts. Results were normalized to cell viability as determined using the MTT assay. Error bars indicate the standard deviation of the mean of 4 replicates from a single experiment. Different letters on the bars signify statistics significance ($p < 0.05$) compared to the untreated control.

more than the basic activities of the transporters (Simpson et al., 2001; Watson et al., 2004; Wang et al., 2020).

5. Conclusion

Phytochemicals are known to play a major role in glucose regulation and in ameliorating hyperglycemia. The findings from the current study showed the presence of important flavonoids, flavonols, and phenolic compounds in the aqueous and ethanol extracts of *H. cymosum*. Both extracts demonstrated potent hypoglycemic, antioxidant, antidiabetic, and anti-inflammatory activities, which play significant roles in the complications of diabetes mellitus. To our understanding, this study was the first to report potential in vitro antidiabetic effects of the aqueous and 70% ethanol extracts of *H. cymosum*. The findings from the plant extracts make them reliable sources of potential plant-based lead compounds for the development of antidiabetic drugs. However, further investigations, especially for the mechanism of actions of these identified phytochemical compounds as well as in vivo studies are recommended.

Funding

This research was funded by Cape Peninsula University of Technology, grant no CPUT-RJ23 granted to OO Oguntibeju.

CRediT authorship contribution statement

Achasih Quinta Nkemzi: Writing – original draft, Software, Methodology, Investigation, Formal analysis, Data curation, Conceptualization. **Kunle Okaiyeto:** Writing – review & editing, Methodology, Data curation. **Nasifu Kerebba:** Writing – review & editing, Formal analysis, Data curation. **Fanie Rautenbach:** Writing – review & editing, Methodology, Formal analysis. **Omolola Oyenihi:** Writing – review & editing, Methodology, Formal analysis. **Okobi Eko Ekpo:** Writing – review & editing, Visualization, Supervision, Methodology, Investigation, Conceptualization. **Oluwafemi O. Oguntibeju:** Writing – review & editing, Visualization, Supervision, Project administration, Methodology, Investigation, Funding acquisition, Conceptualization.

Declaration of competing interest

The authors declare that they have no known conflict of interest financially or personal relationship that could possibly influence the work in the manuscript.

Acknowledgments

The authors acknowledge the financial support (CPUT bursary) and funding by Cape Peninsula University of Technology.

References

Abd Ghafar, S.Z., Mediani, A., Maulidiani, M., Rudiyanto, R., Ghazali, H.M., Ramli, N.S., Abas, F., 2020. Complementary NMR-and MS-based metabolomics approaches reveal the correlations of phytochemicals and biological activities in *Phyllanthus acidus* leaf extracts. Food Res. Int. 136, 109312.

Abifarin, T.O., Otunola, G.A., Afolayan, A.J., 2021. Cytotoxicity, anti-obesity and anti-diabetic activities of *Heteromorpha arborescens* (Spreng.) Cham Leaves. Processes 9, 1671.

Abu-Reidah, I.M., del Mar Contreras, M., Arráez-Román, D., Fernández-Gutiérrez, A., Segura-Carretero, A., 2014. UHPLC-ESI-QTOF-MS-based metabolic profiling of *Vicia faba* L.(Fabaceae) seeds as a key strategy for characterization in foodomics. Electrophoresis 35, 1571–1581.

Adewinogo, S.O., Sharma, R., Africa, C.W., Marnewick, J.L., Hussein, A.A., 2022. Chemical Study and Comparison of the Biological Activities of the Essential Oils of *Helichrysum petiolare, H. cymosum*, and *H. odoratissimum*. Plants 11, 2606.

Agarwal, P., Gupta, R., 2016. Alpha-amylase inhibition can treat diabetes mellitus. Res. Rev. J. Med. Health Sci. 5, 1–8.

Akinfenwa, A.O., Sagbo, I.J., Makhaba, M., Mabusela, W.T., Hussein, A.A., 2022. *Helichrysum* genus and compound activities in the management of diabetes mellitus. Plants 11, 1386.

Akinyede, K.A., Cupido, C.N., Hughes, G.D., Oguntibeju, O.O., Ekpo, O.E., 2021a. Medicinal properties and In vitro biological activities of selected *Helichrysum* species from South Africa: a review. Plants 10, 1566.

Akinyede, K.A., Hughes, G.D., Ekpo, O.E., Oguntibeju, O.O., 2022. Comparative study of the antioxidant constituents, activities and the GC–MS quantification and identification of fatty acids of four selected Helichrysum species. Plants 11, 998.

Akinyede, K.A., Oyewusi, H.A., Hughes, G.D., Ekpo, O.E., Oguntibeju, O.O., 2021b. In vitro evaluation of the anti-diabetic potential of aqueous acetone *helichrysum petiolare extract* (AAHPE) with molecular docking relevance in diabetes mellitus. Molecules 27, 155.

Al-Mustafa, A., Al-Tawarah, M., Al-Sheraideh, M.S., Al-Zahrany, F.A., 2021. Phytochemical analysis, antioxidant and in vitro β-galactosidase inhibition activities of *Juniperus phoenicea* and *Calicotome villosa* methanolic extracts. BMC Chem. 15, 1–13.

Aladejana, A.E., Bradley, G., Afolayan, A.J., 2020. In vitro evaluation of the anti-diabetic potential of *Helichrysum petiolare* Hilliard & BL Burtt using HepG2 (C3A) and L6 cell lines. F1000Res 9.

Alperth, F., Turek, I., Weiss, S., Vogt, D., Bucar, F., 2019. Qualitative and quantitative analysis of different *Rhodiola rosea* rhizome extracts by UHPLC-DAD-ESI-MSn. Sci. Pharm. 87, 8.

Amoo, S.O., Mudau, T.E., Olowoyo, J.O., 2022. In vitro α-glucosidase inhibitory activity of medicinal plants used traditionally for treating diabetes in Vhembe District, South Africa. J. Herbmed. Pharmacol. 11, 513–521.

Ansari, P., Akther, S., Hannan, J.M.A., Seidel, V., Nujat, N.J., Abdel-Wahab, Y.H., 2022. Pharmacologically active phytomolecules isolated from traditional antidiabetic plants and their therapeutic role for the management of diabetes mellitus. Molecules 27, 4278.

Benoite, T., Vigasini, N., 2021. Antioxidant and antidiabetic activities of ethanolic extract of *Hibiscus sabdariffa* calyx and Stevia rebaudiana leaf. Asian J. Biol. Life Sci. 10, 217–224.

Benzie, I.F., Strain, J.J., 1996. The ferric reducing ability of plasma (FRAP) as a measure of "antioxidant power": the FRAP assay. Anal. Biochem. 239, 70–76.

Bohlmann, F., Ziesche, J., Mahanta, P.K., 1979. Neue chalkon-derivate und humulon-ähnliche verbindungen aus *Helichrysum-arten*. Phytochem 18, 1033–1036.

Chadt, A., Al-Hasani, H., 2020. Glucose transporters in adipose tissue, liver, and skeletal muscle in metabolic health and disease. Pflügers Arch.-Eur. J. Physiol. 472, 1273–1298.

Clifford, M.N., Knight, S., Kuhnert, N., 2005. Discriminating between the six isomers of dicaffeoylquinic acid by LC-MS n. J. Agric. and Food Chem. 53, 3821–3832.

Clifford, M.N., Kuhnert, N., 2022. LC–MS characterization and quantification of known and unknown (poly) phenol metabolites—possible pitfalls and their avoidance. Mol. Nutr. Food Res. 66, 2101013.

Crozier, A., Jaganath, I.B., Clifford, M.N., 2009. Dietary phenolics: chemistry, bioavailability and effects on health. Nat. Prod. Rep. 26, 1001–1043.

Dias, A.L., Rozet, E., Larondelle, Y., Hubert, P., Rogez, H., Quetin-Leclercq, J., 2013. Development and validation of an UHPLC-LTQ-Orbitrap MS method for non-anthocyanin flavonoids quantification in *Euterpe oleracea* juice. Anal. Bioanal. Chem. 405, 9235–9249.

Diaz, P., Jeong, S.C., Lee, S., Khoo, C., Koyyalamudi, S.R., 2012. Antioxidant and anti-inflammatory activities of selected medicinal plants and fungi containing phenolic and flavonoid compounds. Chin. Med. 7, 1–9.

Dilworth, L., Facey, A., Omoruyi, F., 2021. Diabetes mellitus and its metabolic complications: the role of adipose tissues. Int. J. mol. Sci. 22, 7644.

Dirir, A.M., Daou, M., Yousef, A.F., Yousef, L.F., 2022. A review of alpha-glucosidase inhibitors from plants as potential candidates for the treatment of type-2 diabetes. Phytochem. Rev. 21, 1049–1079.

Dumbre, A.S., Chaskar, A.T., Hatpakki, B.C., 2023. Utilization of herbal medication & home remedies in the management of diabetes mellitus type II: a comprehensive review. Int. J.Pharm. Sci. 1, 1. -1.

Erukainure, O.L., 2018. Doctoral dissertation.

Escobar-Avello, D., Lozano-Castellón, J., Mardones, C., Pérez, A.J., Saéz, V., Riquelme, S., von Baer, D., Vallverdú-Queralt, A., 2019. Phenolic profile of grape canes: novel compounds identified by lc-esi-ltq-orbitrap-ms. Molecules 24, 3763.

François, T., Lambert, S.M., Dongmo, J., Michel, P., Gaby, N.M.E., Fabrice, F.B., Zache, N., Henri, A.Z.P., Chantal, M., 2010. Composition, radical scavenging and antifungal activities of essential oils from 3 *Helichrysum* species growing in Cameroon against *Penicillium oxalicum* a yam rot fungi. Afr. J. Agric. Res. 5, 121–127.

Gao, C., Zhao, S., Yagiz, Y., Gu, L., 2018. Static, kinetic, and isotherm adsorption performances of macroporous adsorbent resins for recovery and enrichment of bioactive procyanidins from cranberry pomace. J. Food sci. 83, 1249–1257.

Ghani, U., 2015. *Re*-exploring promising α-glucosidase inhibitors for potential development into oral anti-diabetic drugs: finding needle in the haystack. Eur. J Med. Chem. 103, 133–162.

Giacco, F., Brownlee, M., 2010. Oxidative stress and diabetic complications. Circ. Res. 107, 1058–1070.

González, P., Lozano, P., Ros, G., Solano, F., 2023. Hyperglycemia and oxidative stress: an integral, updated and critical overview of their metabolic interconnections. Int. J. Mol. Sci. 24, 9352.

Gouveia, S.C., Castilho, P.C., 2009. Analysis of phenolic compounds from different morphological parts of *Helichrysum devium* by liquid chromatography with on-line UV and electrospray ionization mass spectrometric detection. Rapid Commun. Mass Spectrom. 23, 3939–3953.

Heyman, H.M., 2013. Identification of anti-HIV Compounds in *Helichrysum* species (Asteraceae) By Means of NMR-based Metabolomic Guided Fractionation. University of Pretoria.
Lv, Y., Hao, J., Liu, C., Huang, H., Ma, Y., Yang, X., Tang, L., 2019. Anti-diabetic effects of a phenolic-rich extract from *Hypericum attenuatum* Choisy in KK-Ay mice mediated through AMPK/PI3K/Akt/GSK3β signaling and GLUT4, PPARγ, and PPARα expression. J. Funct. Food. 61, 103506.
Idris, O.A., Kerebba, N., Horn, S., Maboeta, M.S., Pieters, R., 2023. Phytochemical-based evidence of the health benefits of *Bidens pilosa* extracts and cytotoxicity. Chem. Afr. 6, 1767–1788.
Idris, O.A., Kerebba, N., Horn, S., Maboeta, M.S., Pieters, R., 2024. Comparative phytochemistry using UPLC-ESI-QTOF-MS phenolic compounds profile of the water and aqueous ethanol extracts of *Tagetes minuta* and their cytotoxicity. S. Afr. J. Bot. 164, 50–65.
Jadalla, B.M., Moser, J.J., Sharma, R., Etsassala, N.G., Egieyeh, S.A., Badmus, J.A., Marnewick, J.L., Beukes, D., Cupido, C.N., Hussein, A.A., 2022. In vitro alpha-glucosidase and alpha-amylase inhibitory activities and antioxidant capacity of *Helichrysum cymosum* and *Helichrysum pandurifolium* Schrank constituents. Separations 9, 190.
Jimoh, M.O., Jimoh, M.A., Kerebba, N., Bakare, O.O., Senjobi, C.T., Saheed, S.A., Kadye, R., Prinsloo, E., Laubscher, C.P., 2024. Liquid chromatography–mass spectrometry and xCELLigence real time cell analyzer revealed anticancer and antioxidant metabolites in *Trianthema portulacastrum* L.(Aizoaceae). Phytomed. Plus. 4, 100550.
Joost, H.G., Bell, G.I., Best, J.D., Birnbaum, M.J., Charron, M.J., Chen, Y.T., Doege, H., James, D.E., Lodish, H.F., Moley, K.H., Moley, J.F., 2002. Nomenclature of the GLUT/SLC2A family of sugar/polyol transport facilitators. AJP-Endocrinol. Metab. 282, E974–E976.
Kaur, N., Kumar, V., Nayak, S.K., Wadhwa, P., Kaur, P., Sahu, S.K., 2021. Alpha-amylase as molecular target for treatment of diabetes mellitus: a comprehensive review. Chem. Biol. Drug. Des. 98, 539–560.
Kawamura-Konishi, Y., Watanabe, N., Saito, M., Nakajima, N., Sakaki, T., Katayama, T., Enomoto, T., 2012. Isolation of a new phlorotannin, a potent inhibitor of carbohydrate-hydrolyzing enzymes, from the brown alga Sargassum patens. J. Agri. and Food Chem. 60, 5565–5570.
Kifle, Z.D., Enyew, E.F., 2020. Evaluation of in vivo antidiabetic, in vitro α-amylase inhibitory, and in vitro antioxidant activity of leaves crude extract and solvent fractions of *Bersama abyssinica fresen* (melianthaceae). J. Evid.-Base. Integr. Med. 25, 2515690X20935827.
Leonardi, M., Giovanelli, S., Ambryszewska, K.E., Ruffoni, B., Cervelli, C., Pistelli, L., Flamini, G., Pistelli, L., 2018. Essential oil composition of six *Helichrysum* species grown in Italy. Biochem. Syst. Ecol. 79, 15–20.
Leto, D., Saltiel, A.R., 2012. Regulation of glucose transport by insulin: traffic control of GLUT4. Nat. Rev Mol. Cell Biol. 13, 383–396.
Li, S., Hu, X., Pan, J., Gong, D., Zhang, G., 2021. Mechanistic insights into the inhibition of pancreatic lipase by apigenin: inhibitory interaction, conformational change and molecular docking studies. J. Mol. Liquid. 335, 116505.
Li, X., Chen, S., Zeng, J., Cai, R., Liang, Y., Chen, C., Chen, B., Li, C., 2023. Database-aided UHPLC-Q-orbitrap MS/MS strategy putatively identifies 52 compounds from Wushicha Granule to propose anti-counterfeiting quality-markers for pharmacopoeia. Chin. Med. 18, 116.
Lin, D., Xiao, M., Zhao, J., Li, Z., Xing, B., Li, X., Kong, M., Li, L., Zhang, Q., Liu, Y., Chen, H., 2016. An overview of plant phenolic compounds and their importance in human nutrition and management of type 2 diabetes. Molecules 21, 1374.
Liu, T.T., Liu, X.T., Chen, Q.X., Shi, Y., 2020. Lipase inhibitors for obesity: a review. Biomed. Pharmacother. 128, 110314.
López-Cobo, A., Gómez-Caravaca, A.M., Pasini, F., Caboni, M.F., Segura-Carretero, A., Fernández-Gutiérrez, A., 2016. HPLC-DAD-ESI-QTOF-MS and HPLC-FLD-MS as valuable tools for the determination of phenolic and other polar compounds in the edible part and by-products of avocado. LWT. 73, 505–513.
Lourens, A.C.U., Van Vuuren, S.F., Viljoen, A.M., Davids, H., Van Heerden, F.R., 2011. Antimicrobial activity and in vitro cytotoxicity of selected South African Helichrysum species. S. Afri. J. Bot. 77, 229–235.
Lourens, A.C.U., Viljoen, A.M., Van Heerden, F.R., 2008. South African *Helichrysum* species: a review of the traditional uses, biological activity and phytochemistry. J. Ethnopharmacol. 119, 630–652.
Lu, Y., Zhou, W., Feng, Y., Li, Y., Liu, K., Liu, L., Lin, D., He, Z., Wu, X., 2017. Acteoside and acyl-migrated acteoside, compounds in chinese kudingcha tea, inhibit α-amylase in vitro. J. Med. Food 20, 577–585.
Maniruzzaman, M., Rahman, M.J., Ahammed, B., Abedin, M.M., 2020. Classification and prediction of diabetes disease using machine learning paradigm. Health Inf. Sci. Syst. 8, 1–14.
Maroyi, A., 2019. *Helichrysum cymosum* (L.) D. Don (Asteraceae): medicinal uses, chemistry, and biological activities. Asian J. Pharm. Clin. Res. 12, 19–26.
Martín, C., Martínez, R., Navarro, R., Ruiz-Sanz, J.I., Lacort, M., Ruiz-Larrea, M.B., 2001. tert-Butyl hydroperoxide-induced lipid signaling in hepatocytes: involvement of glutathione and free radicals. Biochem. Pharmacol. 62, 705–712.
Martin, M.A., Ramos, S., Mateos, R., Granado Serrano, A.B., Izquierdo-Pulido, M., Bravo, L., Goya, L., 2008. Protection of human HepG2 cells against oxidative stress by cocoa phenolic extract. J. Agric. Food Chem. 56, 7765–7772.
Matanzima, Y., 2014. Quantitative and Qualitative Optimization of Antimicrobial Bioactive Constituents of *Helichrysum cymosum* Using Hydroponics Technology. Cape Peninsula University of Technology.
Mazza, G., Fukumoto, L., Delaquis, P., Girard, B., Ewert, B., 1999. Anthocyanins, phenolics, and color of Cabernet franc, Merlot, and Pinot noir wines from British Columbia. J. Agric. Food Chem. 47, 4009–4017.
Mcmurrough, I., Mcdowell, J., 1978. Chromatographic separation and automated analysis of flavanols. Anal. Biochem. 91, 92–100.
Mohamed, A.S., Mohamed, O.G., El Shamy, A.M., El Sakhawy, F.S., Al-Karmalawy, A.A., Tripathi, A., El Gedaily, R.A., 2024. Anti-Alzheimer activity and UHPLC-MS based molecular networking of *Pseudobombax ellipticum* cultivars coupled to multivariate data analysis and in silico molecular docking. Egypt. J. Chem. 67, 357–377.
Moriasi, G.A., Kibiti, C.M., Ngugi, M.P., 2021. In Vivo Antidiabetic Efficacy, Mineral Element Composition, and Qualitative Phytochemistry of the Aqueous Leaf Extracts of Pentas Zanzibarica (Klotzsch.) Vatke and Olea Europaea Subspecies Africana (Mill.).
Nasab, S.B., Homaei, A., Pletschke, B.I., Salinas-Salazar, C., Castillo-Zacarias, C., Parra-Saldívar, R., 2020. Marine resources effective in controlling and treating diabetes and its associated complications. Process Biochem. 92, 313–342.
Nethengwe, M., Kerebba, N., Okaiyeto, K., Opuwari, C.S., Oguntibeju, O.O., 2024. Antioxidant, anti-diabetic, and anti-inflammation activity of *Garcinia livingstonei* aqueous leaf extract: a preliminary study. Int. J. Mol. Sci. 25, 3184.
Nemudzivhadi, V., Masoko, P., 2014. In vitro assessment of cytotoxicity, antioxidant, and anti-inflammatory activities of *Ricinus communis* (Euphorbiaceae) leaf extracts. Evid.-Based Complement. Alternat. Med. 2014.
Nešović, M., Gašić, U., Tosti, T., Horvacki, N., Šikoparija, B., Nedić, N., Blagojević, S., Ignjatović, L., Tešić, Ž., 2020. Polyphenol profile of buckwheat honey, nectar and pollen. RS Open Sci. 7, 201576.
Norfaizah, M., 2020. Doctoral dissertation. Universiti Malaya.
Oboh, G., Nwokocha, K.E., Akinyemi, A.J., Ademiluyi, A.O., 2014. Inhibitory effect of polyphenolic–rich extract from *Cola nitida* (Kolanut) seed on key enzyme linked to type 2 diabetes and Fe2+ induced lipid peroxidation in rat pancreas in vitro. Asian Pac. J. Trop.Biomed. 4, S405–S412.
Oguntibeju, O.O., 2019. Type 2 diabetes mellitus, oxidative stress and inflammation: examining the links. Int. J. Physiol. Pathophysiol. and pharmacol. 11, 45.
Okaiyeto, K., Kerebba, N., Rautenbach, F., Singh, S.K., Dua, K., Oguntibeju, O.O., 2022a. UPLC-ESI-QTOF-MS phenolic compounds identification and quantification from ethanolic extract of: in vitro antioxidant and antidiabetic potentials. Arab. J. Chem.
Okaiyeto, K., Kerebba, N., Oguntibeju, O.O., 2022b. UPLC-ESI-QTOF-MS profiling of phenolic compounds from *Eriocephalus africanus*: in vitro antioxidant, antidiabetic, and anti-inflammatory potentials. Molecules 27, 8912.
Olabiyi, F.A., Aboua, Y.G., Popoola, O.K., Monsees, T.K., Oguntibeju, O.O., 2020. Evaluation of antioxidant, antityrosinase activities and cytotoxic effects of *Phyllanthus amarus* extracts. Nat. Prod. J. 10, 130–138.
Olaokun, O.O., Mkolo, N.M., Mogale, M.A., King, P.H., 2017. Phytochemical screening, antioxidant, anti-inflammatory and glucose utilization activities of three South African plants used traditionally to treat diseases. Biol. Med. (Aligarh) 9, 2.
Omodanisi, E.I., Aboua, Y.G., Oguntibeju, O.O., 2017. Assessment of the anti-hyperglycaemic, anti-inflammatory and antioxidant activities of the methanol extract of *Moringa oleifera* in diabetes-induced nephrotoxic male wistar rats. Molecules 22, 439.
Otang, W.M., Grierson, D.S., Ndip, R.N., 2012. Phytochemical studies and antioxidant activity of two South African medicinal plants traditionally used for the management of opportunistic fungal infections in HIV/AIDS patients. BMC Complem. Analtern. Med. 12, 1–7.
Palomino, O.M., Giordani, V., Chowen, J., Fernández-Alfonso, M.S., Goya, L., 2022. Physiological doses of oleic and palmitic acids protect human endothelial cells from oxidative stress. Molecules 27, 5217.
Papachristoforou, E., Lambadiari, V., Maratou, E., Makrilakis, K., 2020. Association of glycemic indices (hyperglycemia, glucose variability, and hypoglycemia) with oxidative stress and diabetic complications. J. Diabet. Res. 2020, 7489795.
Pereira, R.M., Moura, L.P.D., Muñoz, V.R., Silva, A.S.R.D., Gaspar, R.S., Ropelle, E.R., Pauli, J.R., 2017. Molecular mechanisms of glucose uptake in skeletal muscle at rest and in response to exercise. Motriz: Rev Educ. Fís. 23, e101609.
Pimpley, V., Patil, S., Srinivasan, K., Desai, N., Murthy, P.S., 2020. The chemistry of chlorogenic acid from green coffee and its role in attenuation of obesity and diabetes. Prep. Biochem. Biotechnol. 50, 969–978.
Prasathkumar, M., Becky, R., Anisha, S., Dhrisya, C., Sadhasivam, S., 2022. Evaluation of hypoglycemic therapeutics and nutritional supplementation for type 2 diabetes mellitus management: an insight on molecular approaches. Biotechnol. Lett. 44, 203–238.
Pringle, N.A., van de Venter, M., Koekemoer, T.C., 2021. Comprehensive in vitro antidiabetic screening of *Aspalathus linearis* using a target-directed screening platform and cellomics. Food Funct. 12, 1020–1038.
Proença, C., Ribeiro, D., Freitas, M., Fernandes, E., 2022. Flavonoids as potential agents in the management of type 2 diabetes through the modulation of α-amylase and α-glucosidase activity: a review. Criti. Rev. Food Sci. Nutr. 62, 3137–3207.
Ramkumar, K.M., Thayumanavan, B., Palvannan, T., Rajaguru, P., 2010. Inhibitory effect of *Gymnema Montanum* leaves on α-glucosidase activity and α-amylase activity and their relationship with polyphenolic content. Med. Chem. Res. 19, 948–961.
Ravipati, A.S., Zhang, L., Koyyalamudi, S.R., Jeong, S.C., Reddy, N., Bartlett, J., Smith, P. T., Shanmugam, K., Münch, G., Wu, M.J., Satyanarayanan, M., 2012. Antioxidant and anti-inflammatory activities of selected Chinese medicinal plants and their relation with antioxidant content. BMC Complement. Alternat. Med. 12, 1–14.
Re, R., Pellegrini, N., Proteggente, A., Pannala, A., Yang, M., Rice-Evans, C., 1999. Antioxidant activity applying an improved ABTS radical cation decolorization assay. Free radic. Biol. Med. 26, 1231–1237.
Sadiq, I.Z., 2023. Free radicals and oxidative stress: signaling mechanisms, redox basis for human diseases, and cell cycle regulation. Curr. Mol. Med. 23, 13–35.
Sagbo, I.J., Hussein, A.A., 2022. Antidiabetic medicinal plants used in the Eastern Cape Province of South Africa: an updated review. Processes 10, 1817.

Satoh, T., 2014. Molecular mechanisms for the regulation of insulin-stimulated glucose uptake by small guanosine triphosphatases in skeletal muscle and adipocytes. Int. J. Mol. Sci. 15, 18677–18692.
Savova, M.S., Mihaylova, L.V., Tews, D., Wabitsch, M., Georgiev, M.I., 2023. Targeting PI3K/AKT signaling pathway in obesity. Biomed. Pharmacother. 159, 114244.
Sayem, A.S.M., Arya, A., Karimian, H., Krishnasamy, N., Ashok Hasamnis, A., Hossain, C. F., 2018. Action of phytochemicals on insulin signaling pathways accelerating glucose transporter (GLUT4) protein translocation. Molecules 23, 258.
Schram, K., Miketova, P., Slanina, J., Humpa, O., Taborska, E., 2004. Mass spectrometry of 1, 3-and 1, 5-dicaffeoylquinic acids. J. Mass Spectrom. 39, 384–395.
Sharma, O.P., Bhat, T.K., 2009. DPPH antioxidant assay revisited. Food Chem. 113, 1202–1205.
Shauli, M.M., Macingwana, L., Rusike, C.R., 2023. In Vitro Immunomodulation of RAW 264.7 Macrophages by Medicinal Plants used Traditionally to Treat Pulmonary Tuberculosis in South Africa.
Simpson, F., Whitehead, J.P., James, D.E., 2001. GLUT4–at the cross roads between membrane trafficking and signal transduction. Traffic 2, 2–11.
Singh, A., Kumar, S., Kumar, B., 2018. LC-MS identification of proanthocyanidins in bark and fruit of six terminalia species. Nat. Prod. Commun. 13, 1934578X1801300511.
Singleton, V.L., Orthofer, R., Lamuela-Raventós, R.M., 1999. [14]Analysis of total phenols and other oxidation substrates and antioxidants by means of folin-ciocalteu reagent. In Method. Enzymol. 299, 152–178.
Sohn, E.H., Koo, H.J., Hang, D.T.T., Jang, S.A., Namkoong, S., Lim, J.D., Kang, S.C., 2013. Protective effects of ellagic acid on ethanol-induced toxicity in hepatic HepG2 cells. Mol. Cell. Toxicol. 9, 249–256.
Soto Mayer, L., 2019. Phytochemical Analysis of the Methanolic Extract of Tigernut, Tuber of Cyperus esculentus, by Ultra-High Performance Liquid Chromatography Coupled with Electrospray Ionization-Quadrupole-Time of Flight-Mass Spectrometry (UHPLC/ESI-Q-TOF-MS).
Tian, R., Yang, W., Xue, Q., Gao, L., Huo, J., Ren, D., Chen, X., 2016. Rutin ameliorates diabetic neuropathy by lowering plasma glucose and decreasing oxidative stress via Nrf2 signaling pathway in rats. Eur. J. Pharmacol. 771, 84–92.
Tourabi, M., Metouekel, A., Ghouizi, A.E., Jeddi, M., Nouioura, G., Laaroussi, H., Hosen, M.E., Benbrahim, K.F., Bourhia, M., Salamatullah, A.M., Nafidi, H.A., 2023. Efficacy of various extracting solvents on phytochemical composition, and biological properties of *Mentha longifolia* L. leaf extracts. Sci. Rep. 13, 18028.
Tran, N., Pham, B., Le, L., 2020. Bioactive compounds in anti-diabetic plants: from herbal medicine to modern drug discovery. Biol. 9, 252.
Van de Venter, M., Roux, S., Bungu, L.C., Louw, J., Crouch, N.R., Grace, O.M., Maharaj, V., Pillay, P., Sewnarian, P., Bhagwandin, N., 2008. Antidiabetic screening and scoring of 11 plants traditionally used in South Africa. J. Ethnopharmacol. 119, 81–86.
Van Vuuren, S.F., Viljoen, A.M., Van Zyl, R.L., Van Heerden, F.R., Başer, K.H.C., 2006. The antimicrobial, antimalarial and toxicity profiles of helihumulone, leaf essential oil and extracts of *Helichrysum cymosum* (L.) D. Don subsp. cymosum. S. Afr. J. Bot. 72, 287–290.
Visvanathan, R., Houghton, M.J., Williamson, G., 2021. Maltoheptaoside hydrolysis with chromatographic detection and starch hydrolysis with reducing sugar analysis: comparison of assays allows assessment of the roles of direct α-amylase inhibition and starch complexation. Food Chem. 343, 128423.
Vongsak, B., Sithisarn, P., Gritsanapan, W., 2012. HPLC quantitative analysis of three major antioxidative components of *Moringa oleifera* leaf extracts. Planta Med. 78, PJ15.
Wallace, T.C., Giusti, M.M., 2010. Evaluation of parameters that affect the 4-dimethylaminocinnamaldehyde assay for flavanols and proanthocyanidins. J. Food Sci. 75, C619–C625.
Wang, T., Wang, J., Hu, X., Huang, X.-J., Chen, G.-X., 2020. Current understanding of glucose transporter 4 expression and functional mechanisms. World J. Biochem. 11, 76.
Wang, X., Li, Q., Han, X., Gong, M., Yu, Z., Xu, B., 2021. Electroacupuncture alleviates diabetic peripheral neuropathy by regulating glycolipid-related GLO/AGEs/RAGE Axis. Front. Endocrinol. 12, 655591.
Watson, R.T., Kanzaki, M., Pessin, J.E., 2004. Regulated membrane trafficking of the insulin-responsive glucose transporter 4 in adipocytes. Endocr. Rev. 25, 177–204.
Wen, L., You, L., Yang, X., Yang, J., Chen, F., Jiang, Y., Yang, B., 2015. Identification of phenolics in litchi and evaluation of anticancer cell proliferation activity and intracellular antioxidant activity. Free Radic. Biol. Med. 84, 171–184.
Wolfe, K.L., Liu, R.H., 2007. Cellular antioxidant activity (CAA) assay for assessing antioxidants, foods, and dietary supplements. J. Agric. food chem. 55, 8896–8907.
Yang, H.-C., Yu, H., Ma, T.-H., Tjong, W.-Y., Stern, A., Chiu, D.T.-Y., 2020. tert-Butyl Hydroperoxide (tBHP)-induced lipid peroxidation and embryonic defects resemble glucose-6-phosphate dehydrogenase (G6PD) deficiency in C. elegans. Int. J. Mol. Sci. 21, 8688.
Yang, J., Yao, L., Gong, K., Li, K., Sun, L., Cai, W., 2022. Identification and quantification of chlorogenic acids from the root bark of *Acanthopanax gracilistylus* by UHPLC-Q-exactive orbitrap mass spectrometry. ACS Omega 7, 25675–25685.
Zubarev, R.A., Makarov, A., 2013. Orbitrap Mass Spectrometry. ACS Publications.
Zhang, H., Wang, G., Beta, T., Dong, J., 2015. Inhibitory properties of aqueous ethanol extracts of propolis on alpha-glucosidase. Evid. Base. Complement. Altern. Med. 2015 (1), 587383.